# A MODEL FOR THERMOLUMINESCENCE FROM SILICON NANOSTRUCTURES


By

NEBIYU GEMECHU

A THESIS SUBMITTED IN PARTIAL FULFILLMENT OF THE
REQUIREMENTS FOR THE DEGREE OF
MASTER OF SCIENCE IN PHYSICS
AT
ADDIS ABABA UNIVERSITY
ADDIS ABABA,ETHIOPIA
JUNE 2009



nafsif@gmail.com

ADDIS ABABA UNIVERSITY
DEPARTMENT OF
PHYSICS

The undersigned hereby certify that they have read and recommend to the Faculty of Graduate Studies for acceptance a thesis entitled "**A MODEL FOR THERMOLUMINESCENCE FROM SILICON NANOSTRUCTURES**" by **NEBIYU GEMECHU** in partial fulfillment of the requirements for the degree of **Master of Science in Physics**.

Dated: June 2009

Advisor: _____
Dr. Sib Krishna Ghoshal

Examiners: _____
Prof. Malnev V.

_____
Dr. Tesgera B.

ADDIS ABABA UNIVERSITY

Date: **June 2009**

Author: **NEBIYU GEMECHU**

Title: **A MODEL FOR THERMOLUMINESCENCE FROM SILICON NANOSTRUCTURES**

Department: **Physics**

Degree: **M.Sc.** Convocation: **June** Year: **2009**

Permission is herewith granted to Addis Ababa University to circulate and to have copied for non-commercial purposes, at its discretion, the above title upon the request of individuals or institutions.

Signature of Author

# Table of Contents

# Abstract

Light emission from silicon nanocrystallites has received considerable attention in recent years due to its application in field emission and display devices. Most of the bulk materials start showing fascinating behaviors as their size is reduced to nano level.The ability to emit light as a consequence of absorption of energy (luminescence) is one of these behaviors.There are different types of luminescence observed from nanosilicon. One of the different kinds of luminescence is thermoluminescence, which is the emission of light from an insulator or semiconductor when it is heated, that is it is the thermally stimulated emission of light following the previous absorption of energy from radiation. So, there is a direct relationship between temperature and the thermoluminescence intensity. Therefore, in this work, we specifically derive the mathematical expression for the thermoluminescence intensity from silicon quantum dots as function of temperature and size of the dot using two proposed models. We also calculate the activation energy as a function of temperature and size of the dot using our model calculation for activation energy. Some of our results are quite new and requires future studies.

# Acknowledgements

Above all, I would like to thank the almighty God who guided me in his eternal will and helped me in finishing my graduate study.

I would like to thank my advisor as well as instructor Dr. Sib Krishna Ghoshal for his indispensable prompt help and invaluable effort in guiding, supervising, encouraging and providing the necessary materials throughout my graduate study and during the course of this thesis.

It gives me great pleasure to express my great gratitude to Mr. Fekadu Legesse who helped me much in providing me some recent materials for the successful accomplishment of this thesis.

Of course, I am grateful to my family for their patience love, and continuous encouragement during my stay in the graduate program.

I would like to thank my friends Mr. Dilbetigil Assefa and Mr. Gezahegn Sufa for their contributions in making their own office computers free for me.

My sincere thanks also goes to all my friends who gave me fruitful comments and advice while typing this thesis on computer.

I am also grateful to my friends Mr. Yehualawork Getahun and Mr. Kiros Hagos for their help in sending me my salary from my sponsor institution (Mizan-Tepi University).

# Chapter 1

# Introduction

In this chapter we are going to discuss about definition of luminescence, the different types of luminescence, mechanism of luminescence, direct and indirect band-gap silicon nanostructures, and density of states.

## 1.1 Definition of luminescence

Luminescence is the emission of light by a material as a consequence of it absorbing energy. A material that emits light is called luminescent material. The emission of light takes place in a characteristic time t after the absorption of the radiation and this parameter allows us to sub classify the process of luminescence. Thus we can distinguish between fluorescence in which $t < 10^{-8}$ s and phosphorescence in which $t > 10^{-8}$s [1].

To describe light emitting or luminescent material the Greek word 'phosphor' is usually used and it means 'light bearer'. A phosphor is luminescent; that is it emits energy from an excited electron as light. The excitation of the electron is caused by absorption of energy from an external source such as another electron, a photon or an electric field. An excited electron occupies a quantum state whose energy is

above the minimum energy ground state. In semiconductors and insulators, the electronic ground state is commonly referred to electrons in the valence band, which is completely filled with these electrons. The excited quantum state often lies in the conduction band, which is empty and separated from the valence band by gap, $E_g$. Therefore unlike metallic materials, small continuous change in electron energy with in the band is not possible. Instead a minimum energy equal to the band gap energy is necessary to excite an electron in semiconductor and insulator, and the energy released by de-excitation is often nearly equal to the band gap. The band gap of semiconductor material is such that at room temperature, very few electrons are promoted from the valance band to the conduction band leaving holes in the valence band. In general, luminescence emission is explained by the transfer of energy from radiation to the electrons of the solid, thus exciting the electrons from a ground state to an excited state . The emission of a luminescent photon takes place when an excited electron returns to a lower energy state. Thus, for fluorescence, the delay between the two transitions is less than $10^{-8}$ s and this process is temperature independent. But, for phosphorescence the delay in time between the two transitions is greater than $10^{-8}$ s and this process is temperature dependent [1].

When radiation is incident on a material, some of its energy may be absorbed and re-emitted as light of a longer wavelength (stroke's law). This is the process of luminescence. The wavelength of the emitted light is characteristic of the luminescent substance and not of the incident radiation. Usually, most studies of luminescence phenomena are concerned with the emission of visible light, but other wavelengths can be emitted, such as ultra-violet or infra-red.

## 1.2 Types of luminescence

According to the type of radiation used to excite the emission, luminescence can be classified in to different types.

### 1.2.1 Photoluminescence

Photoluminescence is the process in which a substance absorbs photons and radiates photons back out [2]. Quantum mechanically, this can be described as an excitation to a higher energy state and then a return to a lower energy state accompanied by the emission of photon. The period between absorption and emission is typically extremely short, in the order of 10 nanoseconds. Light can be emitted when an electron recombines with hole in the semiconductor. In other words, when an insulator or a semiconductor absorbs electromagnetic radiation (i.e. a photon), an electron may be excited to a higher energy quantum state. If the electron returns (relaxes) to a lower energy quantum state by radiating a photon, the process is called photoluminescence (PL). Some of the quantum state relaxation transitions are not allowed based on the spin selection rules. The PL intensity depends on the measurement temperature and the energy of the exciting light (known as photoluminescence excitation or PLE spectrum). In recent years photoluminescence from silicon nanostructures has attracted much attention [2,3]. Figure 1.1 shows the photoluminescence intensity as function of temperature.

To make photoluminescence efficient the electron and hole must be close enough to each other to have overlapping momentum distributions and hence wave functions. It is observed that photoluminescence efficiency increases following the reduction of material size. One reason for this is the quantum confinement effect. Quantum confinement has the effect of increasing the band gap of a material relative to the bulk value. Therefore, silicon nanocrystals emit in the near-infrared to visible range. In

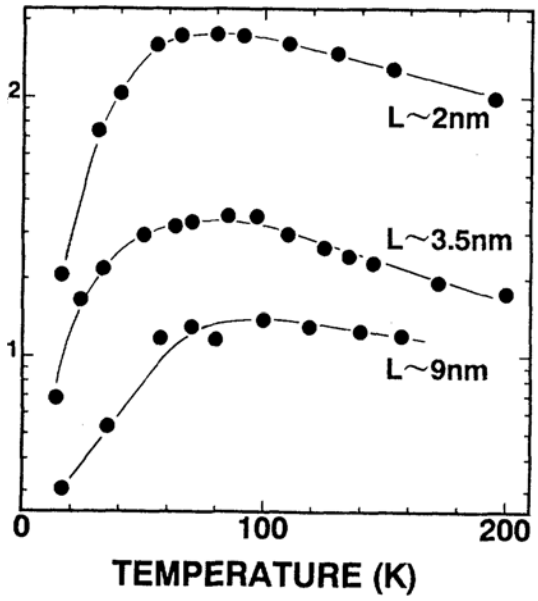


Figure 1.1: Temperature dependence of the PL intensity in porous silicon films of L $\sim$ 2, $\sim$ 3.5 and $\sim$ 9nm. The PL intensity increases with raising the temperature up to about 100 K and the decreases gradually
[4].

these systems, the emission of a photon upon the radiative recombination of quantum-confined excitons occurs at an energy that depends on the nanocrystal size, and the photoluminescence is size-tunable. Quantum confinement leads to an enhancement in the radiative rate. In systems of silicon nanocrystals, one can additionally take advantage of the high quality oxide to passivate the surface and therefore eliminate many non-radiative channels, such as dangling bonds and defect centers. This further enhances the quantum efficiency by reducing the total decay rate. The other reason for enhanced luminescence from silicon nanostructures can be explained in terms of Heisenberg uncertainty principle. According to this principle, when an electron and hole are confined with in the small volume of nanocrystals, their positions are defined to such a degree that their momenta become undetermined [5].

$$\Delta X \Delta P \geq \hbar$$

This implies that the momentum distribution of the electron and hole get smeared out and overlap, enabling light emission.

### 1.2.2 Electroluminescence

When a material emits electromagnetic radiation as a result of the application of an electric field, the process is called electroluminescence (EL) [1].

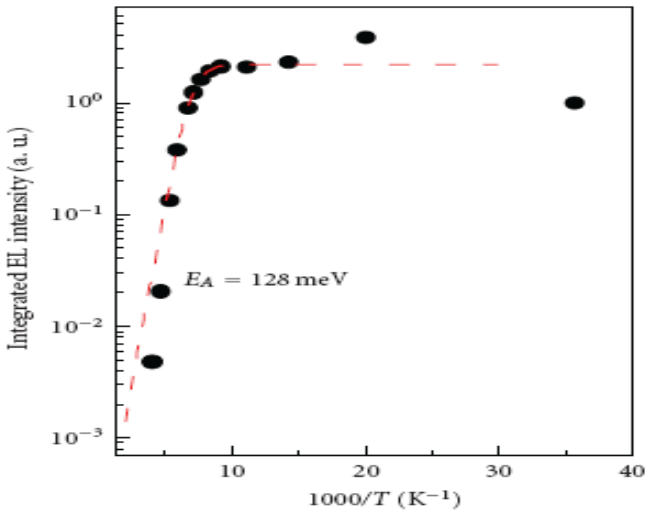


Figure 1.2: EL intensity as a function of the reciprocal temperature for a CVD grown sample. The activation energies obtained from fits to the data (dashed lines) are also shown [6].

The photon emitted results from radiative recombination of electrons and holes created in the phosphor by the voltage between the two electrodes. One of the electrodes is transparent to the wavelength of the light emitted by the device. The first report

of an EL device was in 1907, when Henry Joseph Round observed that light was emitted from silicon carbide under the application of a high voltage. Figure 1.2 shows Electroluminescence intensity as function of the reciprocal temperature.

### 1.2.3 Thermoluminescence

Thermoluminescence is the emission of light from an in insulator or semiconductor when it is heated, that is it is the thermally stimulated emission of light following the previous absorption of energy from radiation [1,7]. There are three essential ingredients necessary for the production of thermoluminescence. Firstly, the material must be an insulator or semiconductor-metals do not exhibit luminescent properties. Secondly, the material must have at some time absorbed energy during exposure to radiation. Thirdly, the luminescence emission is triggered by heating the material. In addition, there is one important property of thermoluminescence. It is a particular characteristic of thermoluminescence that, once heated to excite the light emission, the material can not be made to emit thermoluminescence again by simply cooling the specimen and reheating. In order to re-exhibit the luminescence, the material has to be re-exposed to radiation, whereupon raising the temperature will once again produce light emission [1]. The fundamental principles which govern the production of thermoluminescence are essentially the same as those which govern all luminescence processes, and in this way the thermoluminescence is one of a large family of luminescence phenomena. Figure 1.3 shows the relationships between radiation absorption and the emission of fluorescence, phosphorescence and thermoluminescence.

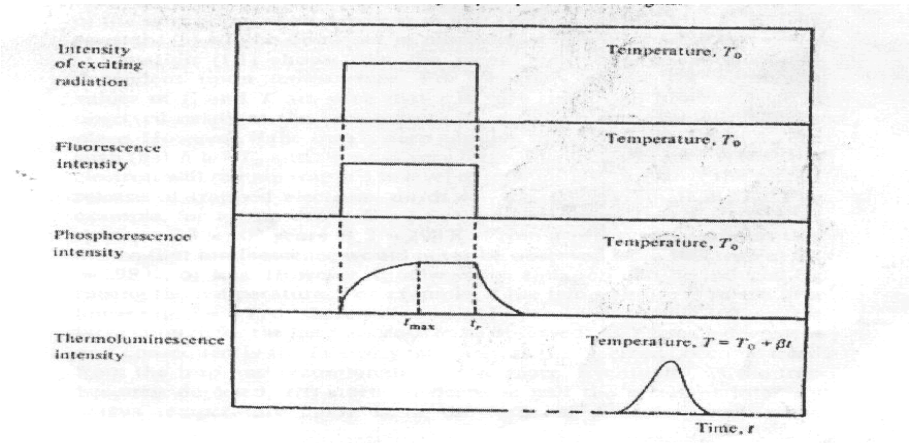


Figure 1.3: Relationships between radiation absorption and the emission of fluorescence, phosphorescence and thermoluminescence. $T_0$ is the temperature at which the irradiation takes place: $\beta$ is the heating rate: $t_r$ is the time at which the irradiation ends and the decay of phosphorescence begins [1].

The following are also other types of luminescence [8].

- Triboluminescence:Triboluminescence is light emission due to mechanical energy
- Chemoluminescence:is generated due to chemical energy
- Bioluminescence:Bioluminescence is generated due to biochemical energy
- chathodoluminescence: emission due to electron beam
- radioluminescence: emission due to nuclear radiations, i.e. gamma rays, beta rays, x-rays etc
- sonoluminescence: emission due to sound waves

## 1.3 Mechanism for luminescence

There is much debate about the photoluminescence (PL) mechanism of the nanoscale silicon or silicon oxide systems containing oxidized porous silicon. For example, the two competitive processes, namely, the quantum confinement (QC) process and the quantum confinement luminescence center(QCLC) processes take place in the PL [9]. The photo excitation occurs in the nanosilicon particles for both of the processes, while the photoemission occurs either in the nanosilicon particles for the QC process or in the luminescence centers (LCs) in silicon oxide adjacent to the nanosilicon particles for the QCLC process. Which process plays the major role in PL is determined by the capture cross-section, the luminescence efficiency, and the density of the luminescent centers and the sizes of the nanosilicon particles. It is generally accepted that the quantum confinement effect (QCE) in the nanocrstallites opens the band gap as well as relaxes the selection rule for radiative transitions, giving rise to above band gap PL in the visible region for crstallites size below $\sim 5nm$ [9,10]. However, QCE alone can not explain the role of various surface treatments and surrounding media. Therefore surface state model should also be taken in to consideration in explaining the photoluminescence mechanism.

Though there is no sufficient information about the mechanism of other types of luminescence, for thermoluminescence it is observed that the the thermoluminescence intensity is inversely proportional to the size of the nanocrystallites [11]. Therefore as the size of the nanocrstallites decreases the thermoluminescence intensity increases. This indicates that the quantum confinement effect plays a major role on the thermoluminescence efficiency and it can be taken as one model to explain the thermoluminescence mechanism from silicon nanostructures [11,12].

## 1.4 Direct and indirect band-gap silicon nanostructures

Silicon is the most prevalent material in the electronics world, not only because of its abundance and low cost, but also because it has a high-quality, stable oxide that provides excellent electronic passivation. However, due to its indirect band gap, the electronic structure of silicon prevents this material from being a strong light emitter. In indirect band gap semiconductors like silicon, there is a mismatch in momentum space between the electron and hole states. To conserve momentum, excitation and relaxation between the conduction band and valence band extrema require the assistance of a crystal lattice vibration. Radiative recombination of excited charge carriers is therefore a three-body process, and, as a result, it is much less efficient than the analogous two-body recombination in a direct band gap semiconductor, where the conduction and valence band extrema are matched in momentum space. The low probability of radiative recombination in indirect band gap materials favors non-radiative decay processes, and excited electrons generally lose energy as heat, not emitted photons. These materials exhibit only very faint luminescence, even at low temperatures, and this weakness has traditionally prevented the desirable extension of silicon microelectronics to silicon optoelectronics; LEDs and lasers cannot be produced from bulk silicon [13].

In the direct band gap semiconductors (as shown in the figure 1.5), the positions of the highest energy state of the valence band (HOMO-highest occupied molecular orbital) and the lowest energy state of the largely unoccupied conduction band (LUMO-lowest unoccupied molecular orbital) are at the same k resulting in a high probability of emitting light [13].

In the case of an indirect band gap semiconductor, the valence band maximum and the conduction band minimum are at different values of k. Therefore electrons need

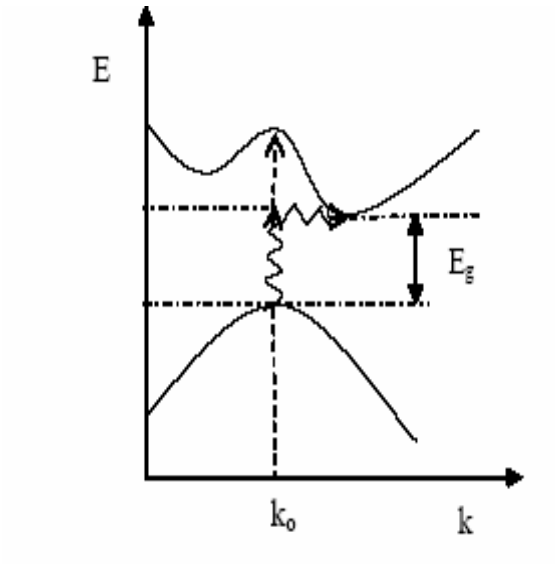


Figure 1.4: Indirect transitions between valance band and conduction band [14].

to undergo a change in the value of k followed by change in energy. Therefore the transition requires a change in both energy and momentum. In other words, an indirect transition requires energy excitation of an electron simultaneous with an electron-phonon interaction to give the required momentum change. Therefore the absorption and recombination efficiency of direct band gap material is about four orders of magnitude larger than that of indirect material. Figure 1.6 shows the effect of the size of nanostructured material on band gap.

Very recently, many attempts have been made to produce quasi-direct gap semiconductor nanostructures and a great deal of research efforts are focused on nanometer-size crystallites or quantum dots made from silicon or germanium. Strong photoluminescence (PL) from silicon nanostructures produced by electrochemical anodization, often called porous silicon, has attracted much attention from fundamental physics viewpoint and because of the potential application to optical devices.

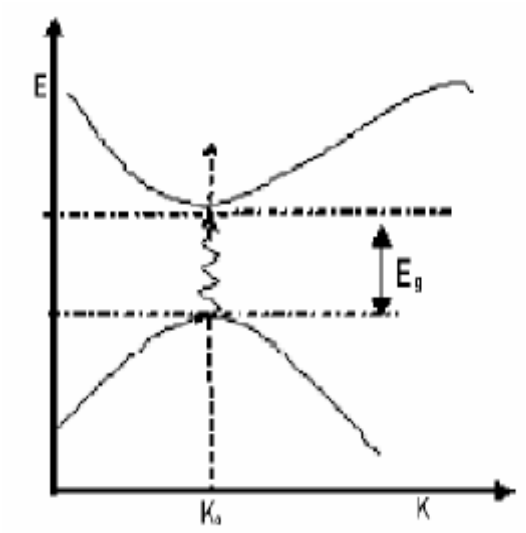


Figure 1.5: Direct transitions between valance band and conduction band [14].

## 1.5 Density of states

In order to characterize the physical properties like optical transitions, charge transport etc., the information about the density of states is very crucial [16]. The density of states depends on the dimensionality of the system and the energy versus the corresponding wavevector dispersion relation for the system at hand [16,17]. A general expression for the density of states valid for all types of materials is as a sum delta functions

$$g(E) = \Sigma\delta(E - E_i), \tag{1.5.1}$$

or

$$g(w) = \Sigma\delta(w - w_k). \tag{1.5.2}$$

For parabolic approximation of the energy versus the corresponding wavevector dispersion relation for the electron or hole we can take a simpler form. Therefore, for

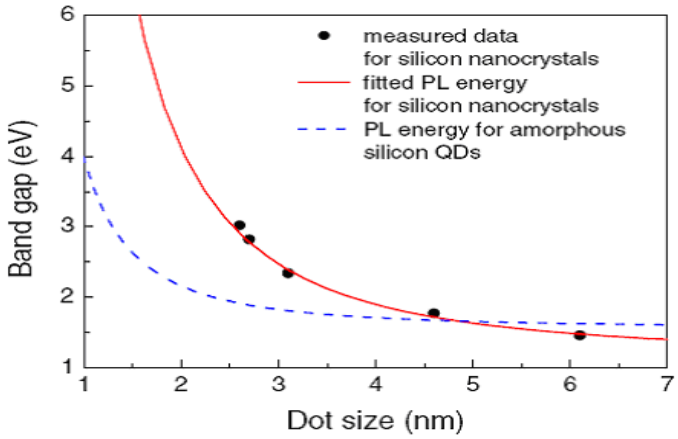


Figure 1.6: Photoluminescence peak energy of silicon nanocrystallites as a function of crystal size [15]. The solid line was obtained from the effective mass theory for three dimensionally confined Silicon nanocrystallites.

a three-dimensional bulk material, the DOS is defined as the number of available electronic states per unit volume per unit energy at energy E and is given by

$$g(E) = \frac{\sqrt{2} m_e^{\frac{3}{2}}}{\pi^2 \hbar^3} E^{\frac{1}{2}} \tag{1.5.3}$$

Passing from three-dimensional bulk to two-dimensional structures, (so called quantum well) the carrier movement is restricted to a plane. Such two-dimensional systems include thin films, layer structures and superlattices. Now the DOS is modified to the number of available electronic states per unit area per unit energy and is given by

$$g(E) = \frac{m_e}{\pi^2 \hbar^2} \tag{1.5.4}$$

Further reduction in the dimensionality of the system ends up in a quantum wire. Examples of such one-dimensional structures include nanotubes, semiconductor nanowires, and nanorods. For a quantum wire the DOS is defined as the availability of electronic

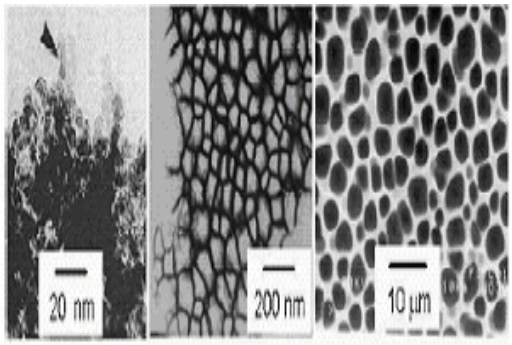


Figure 1.7: Different p-Si structures: nanoporous (left), meso-porous (middle) and macro-porous (right)[11].

states per unit length per unit energy and is given by

$$g(E) = \frac{\sqrt{2m_e}}{\pi\hbar} E^{\frac{-1}{2}} \tag{1.5.5}$$

Finally, for a zero dimensional system (QD), the confinement is along all three dimensions and the DOS becomes a delta function. Figure (1.8) schematically shows the modifications in the DOS as a function of dimension.

Transformation from a 3-D bulk system to a 2-D thin film changes the DOS from a continuous parabolic dependence to a step like dependence. This is due to the quantization of carrier motion in the thickness direction. Consequently the optical absorption edge is shifted to higher energy with respect to the bulk and above the absorption edge; the spectrum is stepped rather than smooth [18].

## 1.6 Objective of the thesis

Apart from giving condensed concept and definitions of the different kinds of luminescence, as discussed in the introduction part, it is much difficult to deal with all the theoretical approaches and basic models for each kind of luminescence in this

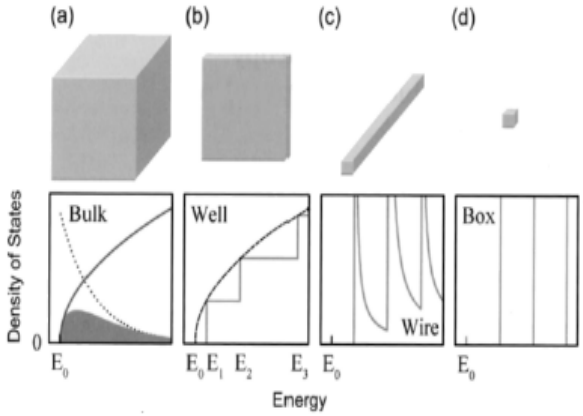


Figure 1.8: Density of states for various geometries of semiconductor materials: (a) 3-D bulk, (b) quantum well, a 2-D structure, (c) quantum wire, a 1-D structure, and (d) quantum dot, a 0-D entity. The dotted line in (a) is the thermal distribution of carriers.

compact thesis. So, we confine ourselves to only one kind of luminescence called thermoluminescence. Therefore, as it will be seen in the following chapters, the main objective of this thesis is to deal with the theoretical models for thermoluminescence from silicon nanostructures in general and to calculate the mathematical expression of the thermoluminescence intensity as function of temperature in particular. We also develop a model for activation energy and calculate it as a function of temperature and nanoparticale size. Finally we will compare our results with the experimental results.

## 1.7 Thesis outline

In this work we make model calculations for TL intensity and activation energy as a function of temperature and the size of the dot. In chapter two we discuss these models in detail. We propose two models for calculating the TL intensity as function

of temperature. The first model depends on the concept of bulk material and the second model directly calculates the number of detrapped (free) electrons per unit volume to obtain the thermoluminescence intensity as function of temperature. We also make one model calculation for the temperature and size dependent activation energy. In chapter three, we review recent experimental results on thermoluminescence from silicon nanostructures. These experimental results will be used to make comparison with our results. In chapter four we use the proposed models to generate our data using FORTRAN code. We also give brief explanation of the results in this chapter. Chapter five gives conclusion and future outlook. Some applications of thermoluminescence will also be discussed in this chapter. Finally the appendix part gives the FORTRAN codes used to generate our data.

# Chapter 2

# Model for thermoluminescence

In this chapter we are going to make a quantitative approach to thermoluminescence. In addition to discussing one model called the simple model for thermoluminescence, we are much interested in proposing our own models for the measurement of thermoluminescence intensity as function of temperature. This much interesting part will be discussed under section 2.5. Under section 2.6 we give brief and condensed description of the comparison of the two models we proposed under section 2.5. In section 2.7, we make detailed calculation for activation energy.

## 2.1 Background of thermoluminescence

According to Becker (1973) medieval alchemists were aware that certain minerals glowed faintly when heated in the dark. However, possibly the first scientifically recorded observation of thermoluminescence was made in 1963 by Robert Boyle. Boyle also stimulated the luminescence emission by more conventional means by using the heat from a hot iron, from friction and from a candle. In 1676, Elsholtz observed a similar effect from the mineral fluorspar. Early interpretations of the phenomena were that the heat itself was being directly converted to light. Oldenburg (1676),

referring to the thermoluminescence of a phosphor called 'phosphorus smaragdinus', wrote that the material received its light 'from the fire itself'. Most of the other observations at the time supported this or similar views. Du Fay (1726) thought that the luminescence was due to 'a sulphur' which actually burned on heating, but later he was to provide what was possibly the first clear evidence that the observed phenomenon (i.e., thermoluminescence) was nothing more than delayed phosphorescence. His experiments on natural quartz showed that the thermoluminescence could be reactivated by exposure of the sample to light. Heat only stimulated the emission, but was not its cause [1].

Deribere (1936) reported that, in 1821, Calloud, a chemist from Annecy in France, discovered that heating sulphate of Quinine produced an intense blue luminescence between 100 and $180^0_C$. This observation was confirmed shortly afterwards by Pelletier. In 1867, Becquerel also reported luminescence from fluorspar as it was heated. It is difficult to pinpoint exactly when the word thermoluminescence was first used in the published literature, but it is certainly used in 1895 by Wiedemann and Schmidt (1895) in what Becker (1974) describes as ' probably the first careful investigation of experimentally radiation-induced thermoluminescence under its modern name' A major difference between the work of weidemann and schmiidt and that of earlier investigators is that these authors induced the thermoluminescence themselves by irradiating the specimens with an electron beam in the laboratory'. This type of thermoluminescence is sometimes referred to as 'artificial' whereas the earlier observations were on natural thermoluminescence, i.e., that induced by natural radioactivity in the environment. Weidemann and Schmidt studied a wide variety of synthetically produced phosphors. However, the fact that the thermoluminescence from natural specimens could be regenerated in the laboratory was first published by Trowbridge and Burbank (1898). These authors drained the natural thermoluminescence from

fluorite by heating it and then re-excited the thermoluminescence by exposing the specimen to X-rays [1].

The connection between phosphorescence and radiation was the subject of extensive examination in the late nineteenth century and the study of radiation-induced thermoluminescence received a boost from Marie Curie in 1904 when she wrote in her doctoral thesis; ' certain bodies, such as fluorite, became luminous when heated; they are thermoluminescent'. Their luminosity disappears after some time, but the capacity of becoming luminous afresh through heat is restored to them by the action of a spark and also by the action of radiation.

## 2.2 Theory of thermoluminescence

An essential feature of thermoluminescence process is the change in occupancy of the various localized energy states. These alterations in the population are implemented by electronic transitions from one energy state to another. Several kinds of transitions are possible and some are shown in the figure 2.1 for both electrons and holes.

Transition (a) is the excitation of valence electron from a host atom in to the conduction band in which state it has enough energy to move freely through the lattice. Thus, transition (a) corresponds to the process of ionization and is a result of the absorption of energy from an external source, e.g., radiation. For every free electron in the conduction band a free hole is left behind in the valence band. Thus ionization creates free electron-hole pairs which may wonder through the crystal until such time as they each in turn arrive, and become localized, at defect centers. This results in the trapping of electrons (transition (b)) and/or of holes (transition (e)). The localized electrons and holes may be released from their traps by thermal excitation (transition (c) and (f)) whereupon they are once again free to move through the crystal.

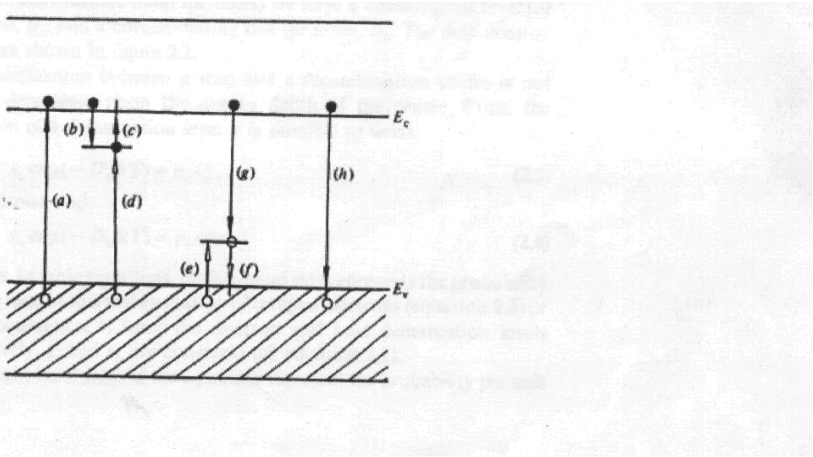


Figure 2.1: Common electronic transitions in crystalline semiconductors and insulators:(a) ionization; (b) and (e) electron and hole trapping respectively; (c) and (f) electron and hole release; (d) and (g) indirect recombination; (h) direct recombination. Electrons, solid circles; electron transitions, solid arrows; holes, open circles; hole transitions, open arrows [1].

A second option open to the free electrons and holes is that they may recombine with a charge carrier of opposite sign, either directly (transition (h)), or indirectly by recombining with a previously trapped carrier (transition (d) and (g)). If either of these recombination mechanisms is accompanied by the emission of light (i.e., it is radiative) then luminescence results. Thus, localized energy levels can act either as traps or as recombination centers and it becomes pertinent to determine what distinguishes a recombination center from a simple trap. The classification which is used to distinguish between the two types is based upon the relative probabilities of recombination and thermal excitation. For the electron trapping center shown in figure 2.1, if transition (c) is more probable than transition (d), then the center is classed as a trap. Conversely, if transition (d) is more probable than transition (c), then the energy level corresponds to a recombination center. Similarly for hole center and transitions (g) and (f).

The probability of charge carrier being thermally released from its trap is exponentially related to $-\frac{E}{KT}$, where E is the 'trap depth', i.e., the energy difference between the trap and the edge of the corresponding delocalized band [1]. Thus, for a given temperature those centers of small E are more likely to be traps than centers of large E. For this reason, recombination centers are located towards the middle of the forbidden gap and traps are located towards the edges. Furthermore, it is possible to see from this how a center which is a trap at one temperature may become a recombination center at lower temperature, and vice versa. This distinguishes between a trap and a recombination center, based on the relative probabilities of trapping and recombination, leads to the possibility that, at a given temperature, there will exist a defect level for which these transition probabilities are equal. Such a level, of depth D, would represent a demarcation between the traps and the recombination centers, such that a center of energy depth E, where $E < D$, would be a trap, whereas if $E > D$, the site would be a recombination center. Because the 'depth' of the trap refers to the energy difference between the localized level and the associated delocalized band (i.e., conduction band for electrons; valence band for holes) we have a demarcation level for electrons, $D_e$, and a corresponding one for holes, $D_h$ [1]. The demarcation levels are shown in figure 2.2.

The distinction between a trap and a recombination center is not simply dependent upon the energy depth of the center. From the definition of a demarcation level it is possible to write

$$S_e \exp(-\frac{D_e}{KT}) = n_r A_r^n \tag{2.2.1}$$

for electrons, and

$$S_h \exp(-\frac{D_h}{KT}) = p_r A_r^p \tag{2.2.2}$$

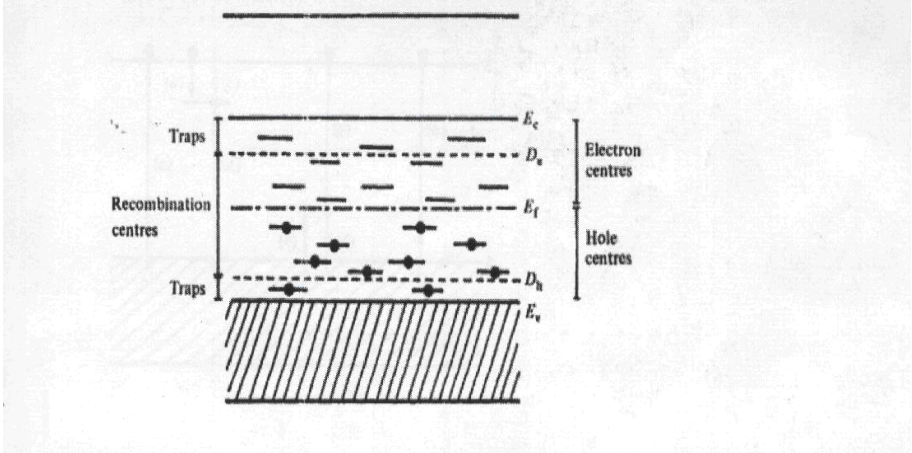


Figure 2.2: Energy levels in an insulator/semiconductor in equilibrium at absolute zero. The levels below $E_f$ are full of electrons, while those above are empty [1].

for holes. In these equations, the left hand-side represents the probability per unit time of thermal excitation of trapped electrons (equation 2.1) or trapped holes (equation 2.2) from the electron and hole demarcation levels respectively. $S_e$ and $S_h$ are constants. The right-hand sides of the equations represent the probability per unit time of recombination of a trapped charge carrier with a free carrier of opposite sign. Here, $n_r$ and $p_r$ are the densities of trapped charge, and $A_r^n$ and $A_r^p$ are the recombination transition coefficients (volume per unit time) for the electrons and holes respectively. Thus, the left-hand sides of equation (2.1) and (2.2) give the probabilities of transitions ( c) and (f) in figure 2.1 and the right-hand sides give the probabilities of transitions (d) and (g). Adirovitch (1956) equates the transition coefficients $A_r^n$ and $A_r^p$ to the products of $v\sigma_r^n$ and $v\sigma_r^p$ respectively. Here $v$ is the thermal velocity of the free carriers in conduction or valence bands and $\sigma_r^n$ and $\sigma_r^p$ are the cross-sections for the capture of the free charges (electrons or holes) by the trapped charges (holes or electrons). Thus, for a given concentration of trapped charge, it is the value of the capture cross-section which determines the probability of recombination [1].

In figure 2.1 transition (c )involves excitation of an electron from a center to the conduction band, whereas transitions (b) and (g) involve capture, by centers, of electrons from the conduction band. Transitions (d), (e) and (f), likewise involve hole transitions into and out of the valence band. However, in many materials electron and hole transitions can occur directly between centers without the carriers being raised in to the conduction and valence bands. In many phosphors transitions of this type are important in thermoluminescence processes.

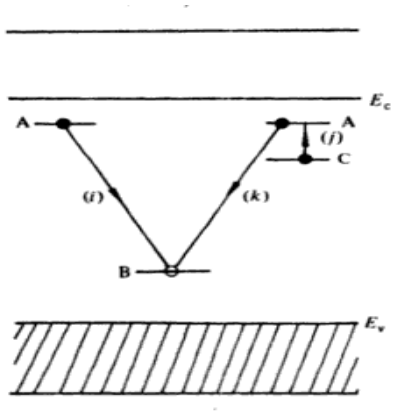


Figure 2.3: Electron transitions in a semiconductor or insulator not involving the conduction or valence bands. Electrons, solid circles; holes, open circles; electron transitions, arrows [1].

Figure 2.3 illustrate the type of center-to-center transition that can take place. In this figure only electron transitions are represented for simplicity. Similar transitions occur for holes. An electron trapped at level A may undergo recombination directly with the hole trapped at B (transition (i)). A recombination of this nature may take place if energy levels of A and B are with in the same atom. If levels A and B are not with in the same atom, a transition of type (i) can take place by tunnelling, if the defects responsible for the levels are situated close to each other in the host lattice

(i.e., few lattice constants). An alternative possibility is that an electron has to be elevated to a higher energy level before recombination with a trapped hole can take place. Thus, in figure 2.3, an electron at level C has to be raised to A (transition (j)) before recombination (transition (k)) can take place.

## 2.3 Recombination processes

Thermoluminescence emission arising from the recombination of free electrons and holes directly across the gap has been observed in a variety of materials. The emission moves to shorter wavelengths as the temperature is reduced and in fact is seen to follow the absorption edge with temperature. Band-to-band transition can occur in two ways. (i) If the minimum of the conduction band and the maximum of the valence band occur at the same value of the wave vector, then the transition can take place without momentum transfer and so the process has relatively high probability. (ii) if the band maxima occur at different wave vectors then momentum transfer must take place which gives the band-to-band transition a low probability. Materials for which the energy band extremes coincide (type i) are called direct-gap materials, whilst those of type (ii) are called indirect-gap materials. The temperature dependence of the life time $\tau$ of a free carrier for direct recombination (i.e., the mean time an electron spends in the conduction band before direct recombination with a free hole in the valence band) was determined and is given by

$$\tau = \frac{n_i}{2R}$$

where $n_i$ is the intrinsic free carrier density and R is the temperature dependent rate of direct recombination. Thus we can write

$$R = \sigma n_i^2 v$$

where $\sigma$ is the direct recombination cross-section [1].

All thermoluminescence phenomena are governed by the process of electron-hole recombination. From figure 2.1 and 2.3 three distinct types of recombination transition are possible, namely, band-to band (transition (h)), band-to center (transition (d) and (g)) and center-to-center (transition (i) and (k)). The band-to-band transition may be termed 'direct', whilst recombination involving localized levels, i.e., the centers, may be termed 'indirect'. Furthermore, in order for luminescence to occur, the recombination must be accompanied by the emission of a photon, i.e., it must be radiative. Thus, it becomes necessary to discuss those factors which govern the relative probabilities of direct and indirect, or radiative and non-radiative processes.

## 2.4 The simple model for thermoluminescence

The simple model of thermoluminescence is shown in the figure 2.4. In this energy band scheme, there are just two localized levels, one situated between the demarcation level and the delocalized band (i.e $D_e$ and $E_c$, or $D_h$ and $E_v$ in figure 2.4) and the other situated somewhere between $D_e$ and $D_h$. Thus, one level acts as trap (T) and the other acts as recombination center (R). In figure 2.2 the trap is situated above the equilibrium Fermi level $E_f$ and thus is empty in the equilibrium state ( i.e before the absorption of radiation). It is therefore a potential electron trap. The recombination center, on the other hand, is situated below the Fermi level and is thus full of electrons and is a potential hole trap.

The absorption of radiation of energy $(h\nu)_a > E_c - E_v$ (i.e greater than the band gap energy results in the ionization of valence electrons, producing free electrons in the conduction band and free holes in the valence band (transition 1). The free carriers may either recombine with each other or become trapped at the trap centers. In

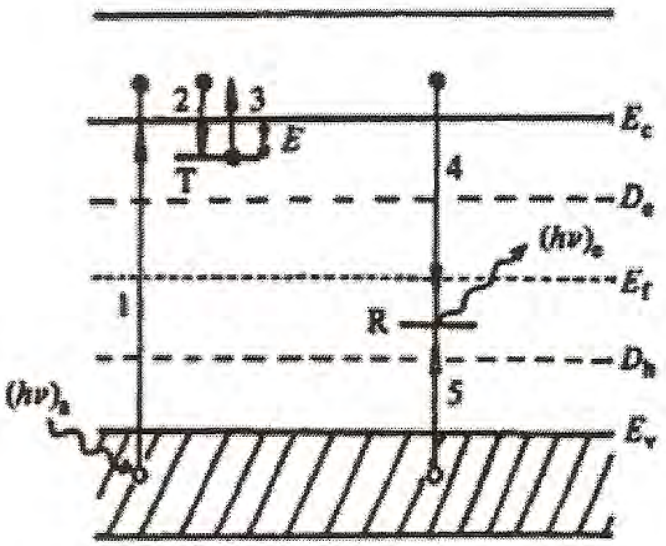


Figure 2.4: Simple two-level model for thermoluminescence. Allowed transition: (1)ionization; (2) and (5) trapping; (3) thermal release; (4) radiative recombination and emission of light [1].

order for recombination to occur holes first become trapped at centers (R) (transition 5). Recombination takes place via the annihilation of the trapped holes by free electrons (transition 4). If, in this model, the recombination transition is assumed to be radiative, then luminescence will result [1,19].

The free electrons may also become trapped at level T (transition 2) in which case recombination can only take place if the trapped electrons absorb enough energy E to be released back to conduction band, from where recombination is possible. Thus, the luminescence emission is delayed by an amount governed by the mean time t spent by the electrons in the trap, given by the Arrhenius equation $p = t^{-1} = sexp(-E/K_BT)$ , where s is trapping parameter. Here p is defined as the probability per unit time of the release of an electron from the trap. If the trap depth E is such that at the

temperature of irradiation $T_o$, $E \gg KT_o$, then, any electron which becomes trapped will remain so for a long period of time, even after the removal of the irradiation there will exist a substantial population of trapped electrons [1]. Furthermore, because the free electrons and holes are created in pairs and are annihilated in pairs, there must exist an equal population of trapped holes at level R. If the temperature of the sample is raised to a higher temperature T such that $E \leq K_B T$, the probability of detrapping p will increase and the electrons will now be released from the trap in to the conduction band. Thermoluminescence now results when the free electrons recombine with the trapped holes. The intensity of thermoluminescence I(t) at any time during the heating is proportional to the rate of recombination of holes and electrons at level R [1,20]. If $n_h$ is the concentration of trapped holes then

$$I(t) = -\frac{d}{dt} n_h$$

As the temperature rises the electrons are released from the trap and recombination takes place reducing the concentration of trapped holes and increasing the thermoluminescence intensity. As the electron traps are progressively emptied the rate of recombination decreases and thus the thermoluminescence intensity decreases accordingly. This Produces the characteristic thermoluminescence peak [1].

Although it is possible to use the rudimentary two level model to describe many of the essential features of thermoluminescence, it is an unfortunate fact that there is not one known phosphor which is believed to possess such a simple energy band scheme. The best evidence for this comes in fact from thermoluminescence itself. For example, in this elementary uncomplicated picture only one thermoluminescence peak should be observed on heating a specimen following its irradiation. Furthermore, the thermoluminescence emission should be of one basic colour.

## 2.5 Our model of thermoluminescence for silicon quantum dots

### 2.5.1 Model 1

If there were no distortion in surface cells of a solid, the minimum energy required to make an electron free from the interior of the solid is

$$E_o = -\varepsilon_f$$

where $\varepsilon_f$ is the Fermi energy. However, with in the surface layer in which the cells are distorted, this distortion will give rise to appreciable electric field, against which an amount of work

$$W_s = \int e\mathbf{E}.\mathbf{dl}$$

must be performed in moving an electron through the layer. Therefore the correct minimum amount of energy required is

$E_o = -\varepsilon_f + W_s$ and $W_s = -e\Phi$, where $\Phi$ is the local value of the electrostatic potential. Therefore, $E_o = -(\varepsilon_f + e\Phi)$.

Consider the idealized case in which a semiconductor is in thermal equilibrium with its surrounding environment. At temperature T, the electronic distribution function is given by the Fermi-Dirac distribution function

$$f(K) = \frac{1}{\exp\frac{\varepsilon_n(K)-\varepsilon_f}{K_BT} + 1}$$

Where $\varepsilon_n(K) = \frac{\hbar^2K^2}{2m_e} - e\Phi$ and $m_e$ is the effective mass of an electron

$$f(K) = \frac{1}{\exp(\frac{\hbar^2K^2}{2m_eK_BT} - \frac{e\Phi+\varepsilon_f}{K_BT}) + 1} \tag{2.5.1}$$

$$f(K) = \frac{1}{\exp(\frac{\hbar^2 K^2}{2m_e K_B T} + \frac{E_o}{K_B T}) + 1} \tag{2.5.2}$$

The electronic current density from the surface (i.e. number of electrons per unit area of the sample) is given by adding the contributions from all electrons with positive

$$V_x = \frac{\hbar K_x}{m_e} \tag{2.5.3}$$

where the positive x-direction is taken to be the direction of normal out of the surface.

$$J = \frac{-2e}{8\Pi^3} \int_0^\infty V(K) f(K) d^3K \tag{2.5.4}$$

$$J = \frac{-e}{4\Pi^3} \int_0^\infty V(K) f(K) d^3K$$

$$J = \frac{-e}{4\Pi^3} \int_0^\infty d^3K \frac{\hbar K_x}{m_e} \exp \frac{-\hbar^2 K^2}{2m_e K_B T} \exp \frac{-E_o}{K_B T} \tag{2.5.5}$$

$$J = \frac{-e\hbar}{4\Pi^3 m_e} \exp \frac{-E_o}{K_B T} \int_0^\infty d^3K K_x \exp \frac{-\hbar^2 K^2}{2m_e K_B T}$$

$$J = \frac{-e\hbar}{4\Pi^3 m_e} \exp \frac{-E_o}{K_B T} \int_0^\infty K_x \exp \frac{-\hbar^2 K_x^2}{2m_e K_B T} dK_x \int_{-\infty}^\infty \exp \frac{-\hbar^2 K_y^2}{2m_e K_B T} dK_y \int_{-\infty}^\infty \exp \frac{-\hbar^2 K_z^2}{2m_e K_B T} dK_z$$

let $\alpha = \frac{\hbar^2}{2m_e K_B T}$

$$J = \frac{-e\hbar}{4\Pi^3 m_e} \exp \frac{-E_o}{K_B T} \int_0^\infty K_x \exp(-\alpha K_x^2) dK_x \int_{-\infty}^\infty \exp(-\alpha K_y^2) dK_y \int_{-\infty}^\infty \exp(-\alpha K_z^2) dK_z$$

but

$$\int_0^\infty K_x \exp(-\alpha K_x^2) dK_x = \frac{1}{2\alpha}$$

$$\int_{-\infty}^\infty \exp(-\alpha K_y^2) dK_y = \int_{-\infty}^\infty \exp(-\alpha K_z^2) dK_z = \sqrt{\frac{\Pi}{\alpha}}$$

Putting these values in to the expression for the current density

$$J = \frac{-e\hbar}{4\Pi^3 m_e} \frac{m_e K_B T}{\hbar^2} \frac{\Pi}{\alpha} \exp \frac{-E_o}{K_B T}$$

$$J = \frac{-e\hbar}{4\Pi^3 m_e} \frac{m_e K_B T}{\hbar^2} \frac{2\Pi m_e K_B T}{\hbar^2} \exp \frac{-E_o}{K_B T}$$

$$J = \frac{-e m_e K_B^2 T^2}{2\Pi^2 \hbar^3} \exp \frac{-E_o}{K_B T} \tag{2.5.6}$$

For nanostructured semiconductor materials (quantum dots, wires or wells), $E_o$ corresponds to the band gap $E_g$. Therefore, the current density is

$$J = \frac{-e m_e K_B^2 T^2}{2\Pi^2 \hbar^3} \exp \frac{-E_g}{K_B T} \tag{2.5.7}$$

Let us now consider a particular situation of detrapping the electrons at trap center T by applying thermal energy. Here the minimum amount of energy required for detrapping is equal to the trap depth E. Therefore the current density due to trapped electrons is given by

$$J = \frac{-e m_e K_B^2 T^2}{2\Pi^2 \hbar^3} \exp \frac{-E}{K_B T} \tag{2.5.8}$$

Since thermoluminescence is due to the annihilation of detrapped (free) electrons with trapped holes at trap center R, the thermoluminescence intensity $I_{th}$ is directly proportional to the recombination rate. But the recombination rate is directly proportional to the number n of detrapped electrons; hence $I_{th}$ is directly proportional to the number of free electrons n. Hence

$$I_{th} \sim n$$

But n can be expressed as $n = AJ$ , where J is the current density due to detrapped electrons and A is the area, which is constant for a given sample. Therefore

$$I_{th} \sim AJ \tag{2.5.9}$$

Another important idea is that the detrapped elctrons may follow two path ways (radiative and non-radiative path ways). But it is electrons that follow radiative path way that contribute to the thermoluminescence intensity. Hence we can conclude that $I_{th}$ is also directly proportional to the rate of radiative recombination $R_{rad}$.

$$I_{th} \sim R_{rad} A J \tag{2.5.10}$$

Once more $I_{th}$ is directly proportional to the probability per unit time p of the release of an electron from the trap.

$$I_{th} \sim p R_{rad} A J \tag{2.5.11}$$

But,

$$p = Sexp(-E/K_B T) \tag{2.5.12}$$

Substituting the expressions for p and J, the thermoluminescence intensity becomes:

$$I_{th} \sim S R_{rad} A \frac{-e m_e K_B^2 T^2}{2\Pi^2 \hbar^3} \exp \frac{-2E}{K_B T} \tag{2.5.13}$$

S is the trapping parameter. For quantum dot (approximately spherical) of well defined size distribution, $A = \Pi d^2$, where d is the size (diameter) of the dot.

$$I_{th} \sim S R_{rad} \Pi d^2 \frac{-e m_e K_B^2 T^2}{2\Pi^2 \hbar^3} \exp \frac{-2E}{K_B T} \tag{2.5.14}$$

But it is found that s varies with temperature like $T^{-b}$, where $-2 < b < 2$ [1]. Taking $b = 1.99$, the expression approximately becomes:

$$I_{th} \sim R_{rad} \Pi d^2 \frac{-e m_e K_B^2}{2\Pi^2 \hbar^3} \exp \frac{-2E}{K_B T} \tag{2.5.15}$$

More precisely,

$$I_{th} \sim C_1 R_{rad} d^2 \exp \frac{-2E}{K_B T} \tag{2.5.16}$$

For a given size, this expression gives the thermoluminescence intensity as function of temperature. Moreover, we found out that the value of b which is preferable for this model to to best fit the experimental result is 1.99.

### 2.5.2 Model 2

Under this model, we first calculate the number n of detrapped (free) electrons per unit volume to obtain the thermoluminescence intensity as function of temperature. At equilibrium,

$$n' = \int D_e(\varepsilon) f_o(\varepsilon) d\varepsilon \tag{2.5.17}$$

where $D_e(\varepsilon)$ is the density of states of electrons and $f_o(\varepsilon)$ is the equilibrium Fermi-Dirac distribution function.

For detrapped electrons,

$$\varepsilon = E + \frac{\hbar^2 K^2}{2m_e}$$

where $m_e$ and E are the usual effective mass of electron and trap depth respectively. At temperature T,

$$n' = \int D_e(\varepsilon) f_o(\varepsilon, T) d\varepsilon \tag{2.5.18}$$

Since the function $f_o(\varepsilon, T)$ sharply depends on $\varepsilon$ grows, it is possible to substitute infinity for the upper limit of integration.

$$f_o(\varepsilon, T) = \frac{1}{\exp \frac{\varepsilon - \varepsilon_f}{K_B T} + 1}$$

Hence,

$$n'(T) = \int_E^{\infty} D_e(\varepsilon) f_o(\varepsilon, T) d\varepsilon \tag{2.5.19}$$

For free electrons,

$\varepsilon = E + \frac{\hbar^2 K^2}{2m_e}$ which implies that $\varepsilon - E = \frac{\hbar^2 K^2}{2m_e}$

Therefore,

$$D(\varepsilon) = \frac{1}{2\Pi^2}(\frac{2m_e}{\hbar^2})^{\frac{3}{2}}\sqrt{\varepsilon - E} \tag{2.5.20}$$

$$n'(T) = \frac{1}{2\Pi^2}(\frac{2m_e}{\hbar^2})^{\frac{3}{2}}\int_E^\infty \frac{\sqrt{\varepsilon - E}}{\exp\frac{\varepsilon-\varepsilon_f}{K_BT}+1}d\varepsilon \tag{2.5.21}$$

Let

$$\frac{\varepsilon - E}{K_BT} = x$$

$$\frac{E - \varepsilon_f}{K_BT} = y$$

$$\frac{\varepsilon - E}{K_BT} = \frac{\varepsilon - E}{K_BT} + \frac{E - \varepsilon_f}{K_BT} = x + y, d\varepsilon = K_BTdx$$

$$n'(T) = \frac{1}{2\Pi^2}(\frac{2m_e}{\hbar^2})^{\frac{3}{2}}((K_BT))^{\frac{3}{2}}\int_0^\infty \frac{\sqrt{x}}{\exp(x+y)+1}dx \tag{2.5.22}$$

For $E - \varepsilon_f \gg K_BT$

$$n'(T) = \frac{1}{2\Pi^2}(\frac{2m_e}{\hbar^2})^{\frac{3}{2}}((K_BT))^{\frac{3}{2}}\int_0^\infty \frac{\sqrt{x}}{\exp(x+y)}dx \tag{2.5.23}$$

$$n'(T) = \frac{1}{2\Pi^2}(\frac{2m_e}{\hbar^2})^{\frac{3}{2}}((K_BT))^{\frac{3}{2}}\exp(-y)\int_0^\infty \sqrt{x}\exp(-x)dx \tag{2.5.24}$$

$$n'(T) = \frac{\sqrt{\Pi}}{2}\frac{1}{2\Pi^2}(\frac{2m_e}{\hbar^2})^{\frac{3}{2}}((K_BT))^{\frac{3}{2}}\exp\frac{-(E-\varepsilon_f)}{K_BT} \tag{2.5.25}$$

But $n'(T) = \frac{n(T)}{V}$, where $n(T)$ is the number of free electrons and V is the volume of the sample.

$$n(T) = Vn'(T) = V\frac{\sqrt{\Pi}}{2}\frac{1}{2\Pi^2}(\frac{2m_e}{\hbar^2})^{\frac{3}{2}}((K_BT))^{\frac{3}{2}}\exp\frac{-(E-\varepsilon_f)}{K_BT} \tag{2.5.26}$$

Now the thermoluminescence intensity $I_{th}$ can be written as,

$$I_{th} \sim PR_{rad}n \tag{2.5.27}$$

Substituting the values of p, $R_{rad}$ and n,

$$I_{th} \sim S\exp\frac{-E}{K_BT}R_{rad}V\frac{\sqrt{\Pi}}{2}\frac{1}{2\Pi^2}(\frac{2m_e}{\hbar^2})^{\frac{3}{2}}((K_BT))^{\frac{3}{2}}\exp\frac{-(E-\varepsilon_f)}{K_BT} \tag{2.5.28}$$

For quantum dot (approximately spherical) of well defined size distribution,

$V = \frac{\Pi d^3}{6}$, where is the diameter of the sample.

$$I_{th} \sim S\exp\frac{-E}{K_BT}R_{rad}\frac{\Pi d^3}{6}\frac{\sqrt{\Pi}}{2}\frac{1}{2\Pi^2}(\frac{2m_e}{\hbar^2})^{\frac{3}{2}}((K_BT))^{\frac{3}{2}}\exp\frac{-(E-\varepsilon_f)}{K_BT} \tag{2.5.29}$$

Again s varies with temperature as $T^{-b}$ where $-2 < b < 2$. Taking $b = -1.5$, the expression becomes:

$$I_{th} \sim \exp\frac{-E}{K_BT}R_{rad}\frac{\Pi d^3}{6}\frac{\sqrt{\Pi}}{2}\frac{1}{2\Pi^2}(\frac{2m_e}{\hbar^2})^{\frac{3}{2}}((K_B))^{\frac{3}{2}}\exp\frac{-(E-\varepsilon_f)}{K_BT} \tag{2.5.30}$$

This equation can approximately be written as,

$$I_{th} \sim R_{rad}\frac{\Pi d^3}{6}\frac{\sqrt{\Pi}}{2}\frac{1}{2\Pi^2}(\frac{2m_e}{\hbar^2})^{\frac{3}{2}}((K_B))^{\frac{3}{2}}\exp\frac{-2E}{K_BT} \tag{2.5.31}$$

More precisely,

$$I_{th} \sim C_2R_{rad}d^3\exp\frac{-2E}{K_BT} \tag{2.5.32}$$

Again for a given size, this expression gives the mathematical expression for the thermoluminescence intensity as function of temperature. Moreover we found out

that the value of b which is preferable for this model to to best fit the experimental result is $-1.5$.

## 2.6 Comparison of the two proposed models

The mathematical expressions for temperature dependent thermoluminescence intensity in the two proposed models are slightly different and it seems that one of the two should be wrong. But actually not!! We should not be surprised and complain much on the slight difference of the two expressions, because we used two different approaches for the two models. In the first model, we tried to derive the expression for $I_{th}$ starting from the concept of the bulk solid and making some possible modifications for the nanostructured material. In the second model, we directly calculated the equilibrium concentration of detrapped electrons and used it in the calculation of the thermoluminrescence intensity. Therefore the two different expressions obtained are due to the two different approaches we made under the two models and hence one does not contradict the other. But best comparison can be made and more useful information can be gathered from the graphs of the two final expressions for $I_{th}$ which will be done in in chapter four, where we make numerical approaches to thermoluminescence and compare our results and graphs with the experimental data. What is most important is that in both models the calculated thermoluminecence intensity is directly proportional to $\exp \frac{-2E}{K_B T}$.

In the first model,

$$I_{th} \sim C_1 R_{rad} d^2 \exp \frac{-2E}{K_B T}$$

In the second model,

$$I_{th} \sim C_2 R_{rad} d^3 \exp \frac{-2E}{K_B T}$$

Therefore, the slight difference in the two mathematical models is only in the value of the constants $C_1$, $C_2$, $R_{rad}$ and $d$. As we are going to see in chapter four, this difference doesn't make significant change on the shape of the graphs of the two models. But for a size greater than $1nm$, model 2 gives more amplified TL intensity because of its $d^3$ dependence.

## 2.7 Our model calculation for activation energy

The temperature required to detrap an electron from a trap center is directly proportional to the depth of the trap center, i.e to the trap depth E and inversely proportional to the probability P of the release of an electron from the trap center for a given temperature.

$$T \sim E \tag{2.7.1}$$

$$T \sim \frac{1}{Sexp\frac{-E}{K_B T}} \tag{2.7.2}$$

This gives

$$E = TSexp\frac{-E}{K_B T} \tag{2.7.3}$$

As mentioned above, S varies with temperature like $T^{-b}$, where $-2 < b < 2$. Using this value of S the above equation becomes:

$$E = T^{1-b} exp\frac{-E}{K_B T} \tag{2.7.4}$$

Taking the logarithm of both sides and multiplying both sides by $K_B T$,

$$K_B T \ln(E) = K_B T \ln(a) - E \tag{2.7.5}$$

Where $a = T^{1-b}$

$$K_B T \ln(a) = E + K_B T \ln(E) \tag{2.7.6}$$

But $\ln(E) = (E-1) - \frac{(E-1)^2}{2} + \frac{(E-1)^3}{3} - \frac{(E-1)^4}{4} + ...$ Taking the first two leading terms in the expansion,

$$\ln(E) \approx (E-1) - \frac{(E-1)^2}{2} \tag{2.7.7}$$

Using this expression for $\ln(E)$

$$K_B T \ln(a) = E + K_B T(E - 1 - \frac{(E-1)^2}{2}) \tag{2.7.8}$$

Rearranging this equation and using $a = T^{1-b}$ gives the following quadratic equation.

$$K_B T E^2 - E(2 + 4K_B T) + 2K_B T(1-b)\ln(T) + 3 = 0 \tag{2.7.9}$$

By ignoring the constants which will appear in the equation, the solution of this equation gives the following temperature dependent activation energy.

$$E = \frac{(4K_B T) + \sqrt{(4K_B T)^2 - 4K_B T(2K_B T(1-b)\ln(T))}}{2K_B T} \tag{2.7.10}$$

Also it is important to note that the wider the band gap, the higher the probability for the trap centers to be located at more deeper centers and hence the higher the probability for activation energy to be higher. Therefore the activation energy is directly proportional to the energy upshift $\Delta E$ due to band gap widening following the reduction in size. Here $\Delta E = \frac{3.73}{d^{1.39}}$, where d is the size of a given sample. Therefore,

$$E \sim (\Delta E)\frac{4K_B T + \sqrt{(4K_B T)^2 - 4K_B T(2K_B T(1-b)\ln(T))}}{2K_B T} \tag{2.7.11}$$

This expression also gives the size dependence of activation energy for a given temperature.

Generally the derived expressions under sections 2.5.1, 2.5.2, and 2.7 will be used in chapter 4 to generate the desired results using FORTRAN code.

# Chapter 3

# Recent experimental results on thermoluminescence

## 3.1 Experimental results on thermoluminescence from porous silicon

The method of thermally stimulated luminescence (TSL) was used to study the contribution of electron states to the recombination properties of the PS layer that allows one to obtain the trap depth of the thermal release of the charge carriers from electron traps. Despite the detailed consideration of photoluminescence (PhL) features in PS, there is the lack of data about thermally stimulated recombination in PS [20]. PS layers were prepared on phosphorus doped, (100) oriented silicon substrates of $4.5\Omega cm$ resistivity and $350\mu m$ thickness. The growing of the porous layers was provided by the anodization in the solution of 48 percentage $HF : C_2H_6O(1 : 2)$ with two regimes: at the constant current density of $20mA/cm^2$ for 15 min and at the discrete subsequence of the currents, namely, 40, 32, 24, 16, and $8mA/cm^2$ for 3 min of each current value. The last formation mode enlarges the PS inhomogeneity. The selected technological regimes allow one to form the material with the porosity within $60per$ to $70per$. The PS powder formed by scrapping from the PS layer that was prepared on the boron doped silicon substrate at the constant current density of $20mA/cm^2$

for 15 min was applied as the third type of pattern.

The low-temperature measurements were performed with the help of the special automatic equipment for optical thermoactivated spectroscopy (temperature range is from 4.2 to $300K$ with an accuracy better than 0.1 K). The samples were mounted in the holder of the optical helium cryostat and after cooling they were irradiated. For excitation, either the white light from a high-pressure $500W$ mercury lamp (the power density is $3W/cm^2$) was used or this light passed through several optical filters. Optical filters allowed one to select the mercury emission peaks of 365, 436, and 546 nm or wide emission band $\lambda \geq 1000nm$ having the power density of 20, 15, and $4mW/cm^2$ and $1.5W/cm^2$, respectively. To observe the TSL effect, the PS patterns were being irradiated at the fixed temperature $T_{ex}$ in the range of $T_{ex} = 4.2$ 200 K for $t_{ex} = 560s$ where $t_{ex}$ is the time. The choice of such an excitation mode is conditioned by the fact that after the sample irradiation at $T_{ex} = 54.2$ K, the TSL intensity increases with the excitation time achieving the saturation at $t_{ex} = 10$ s [20].

The prolongation of $t_{ex}$ does not change either the intensity or the shape of the TSL signal. Then the patterns were kept in the dark at the excitation temperature for 20 min. The point is that, just after the end of the excitation, the long-time decay is observed, the intensity of which drops by law of $I(t) \sim \frac{1}{t}$. After storage of the excited pattern in the dark for 20 min, the intensity of this decay decreases by more than two orders, and we can consider that the isothermal luminescence disappears fully. TSL glow curves were recorded at the uniform heating with the constant rate of $b = 0.15KC^{-1}$. TSL spectra were recorded through the interference filters and detected by the cooled photomultiplier operated in a photon-counting mode. To calculate the trap depth of the thermal release of charge carriers from electron traps, the method of the fractional heating TSL technique was applied. This method allows one to separate the contributions of two effects to TSL intensity: (i) the reduction

of the concentration of the traps filled by the charge carriers and (ii) the increase of probability of the trap release at the sample heating. The method is based on cycling with a large number of small temperature oscillations superimposed on a uniform heating ramp during measurement. Only a part of the traps with close energies are released during these temperature oscillations [20].

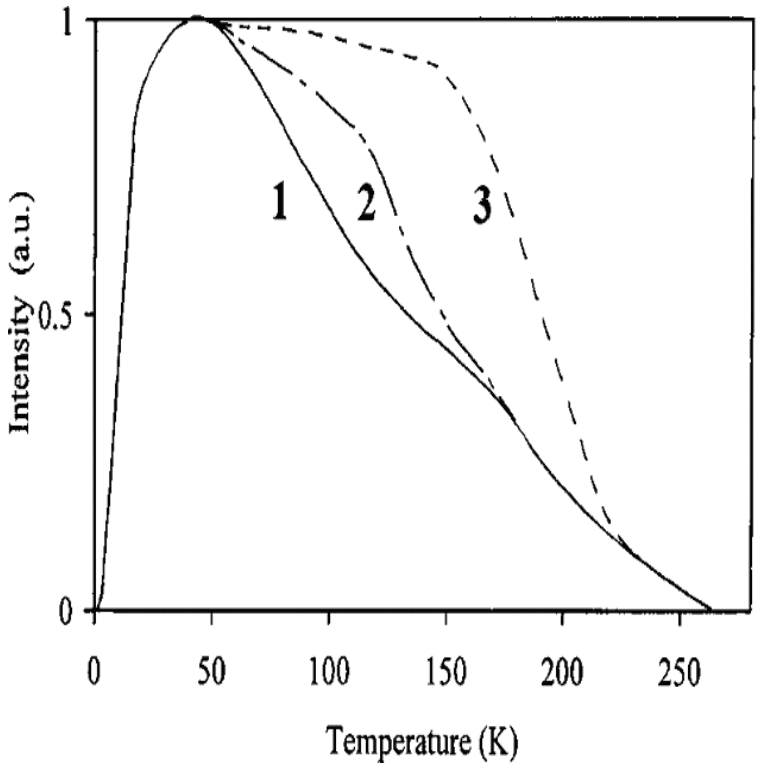


Figure 3.1: The normalized TSL glow curves for PS formed on n-Si at the constant current (1), and at discrete subsequence steps of the currents (2), and for the powder scrapped from PS formed on p-Si (3). $T_{ex}$ = 4.2 K, the excitation by white light for 60 s [20].

The TSL glow curves exhibit the wide weak-structured band in the temperature range from 4.2 to 250 K (Fig.3.1). The weakly expressed maxima are situated at 50, 120, and 160 K. The distribution of intensity in maxima depends on homogeneity

of PS and the type of silicon substrate. Note the observed shape of the TSL signal is typical for disordered amorphous systems, e.g., some polymers, and explained by quasicontinuous spectrum of the electron traps. This conclusion is confirmed by the measurements of temperature dependence of trap depth of the thermal release of traps in PS that was obtained from the fractional TSL technique. Figure 3.2 shows that the activation energy (trap depth) is constant and equal to E' = 0.032 eV at $T < 50K$. The successive temperature growth results in the E(T) increase, and at $T > 70K$, the following linear equation is available [20]:

$$E(T)[eV] = 0.0029T - 0.14$$

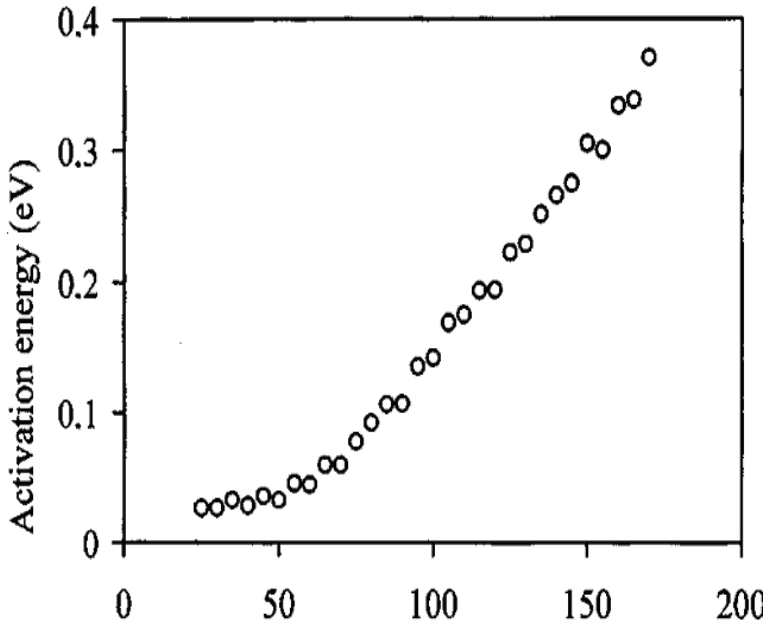


Figure 3.2: The activation energy (trap depth) vs temperature for PS powder [20].

The experimental work has shown the effect of TSL in PS layers. Among other

methods, the TSL offers a powerful tool for evaluation of the deep electron states in the PS band gap. The observed states display the quasicontinuous spectrum having the activation energy (trap depth) from 0.032 to 0.4 eV in the temperature range from 70 to 180 K. The TSL effects as well as PhL can be explained in the framework of the quantum confinement model showing that the localized states play an important role in the radiative recombination in PS. The quantum confinement effects can create the quasicontinuous localized states in band gap that act as electron or hole traps [20].

## 3.2 Importance of the experimental results

In the above section we discussed about the experimental results on thermoluminescence from porous silicon. The experimental techniques used focussed on determining the TL intensity and acivation energy as a function of temperature. It was observed that the TL intensity incsreases with temperature attains its maximum value around 50K and decreases after this temperature. Also it was observed that the activation energy increases with temperature. These experimental results are much important for us to make a comparison with our results. In the next chapter we will write a FORTRAN code and generate our data for the different models discussed in chapter two. Finally we compare our results with the experimental results.

# Chapter 4

# Results and discussions

In this chapter, we make numerical approach to thermoluminescence and write FORTRAN code for the models discussed in chapter two to generate our data.

## 4.1 Results for TL intensity versus temperature: model 1

For model 1, starting from the concept of bulk material we have applied very crucial concepts and have gone through logical steps to reach at the final expression for the temperature dependent thermoluminescence intensity. For a fixed value of b (which is approximately equal to 1.99) the thermoluminescence intensity has a peak value at a temperature of 50K and starts decreasing after this temperature. We have worked for 1-300K temperature range and found out that our result is in good agreement with the experimental results. As it can be seen from the graphs ((a),(b) and (c)), the TL intensity increases with temperature and attains its maximum value near 50K (with sharp peaks) and slowly decreases after this temperature. However, as compared to the experimental result((d)), the TL intensity obtained from this model decays much slower after a temperature of 50K and this may be due to the simplicity of our model.

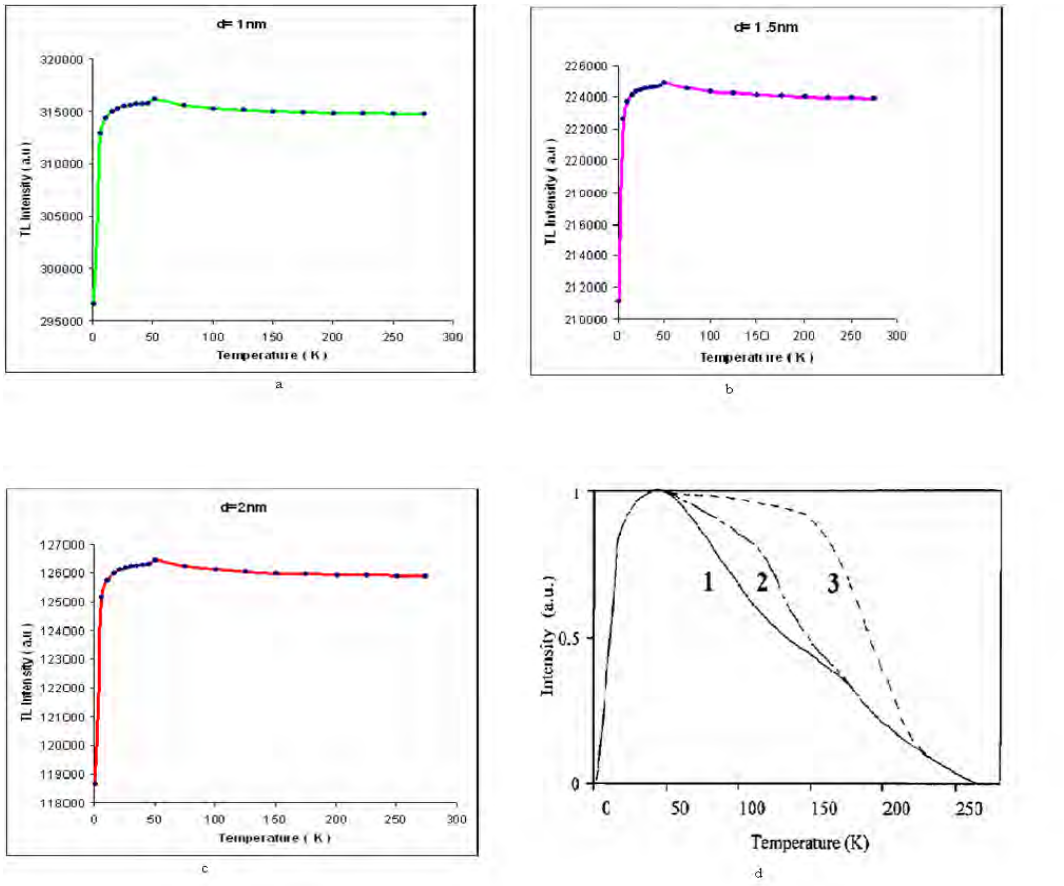


Figure 4.1: The calculated TL intensity for 1nm size (a), 1.5nm size (b), 2nm size (c) and the experimental plot (d): (model 1).

This theoretical model is in good agreement with the experimental results for temperatures lower than 1K. For such lower temperatures, the exponential term approaches zero and hence the TL intensity drops to zero.

## 4.2 Results for TL intensity versus temperature: model 2

For model 2, we directly calculated the number n of detrapped (free) electrons per unit volume (at equilibrium) to obtain the thermoluminescence intensity as function of temperature.

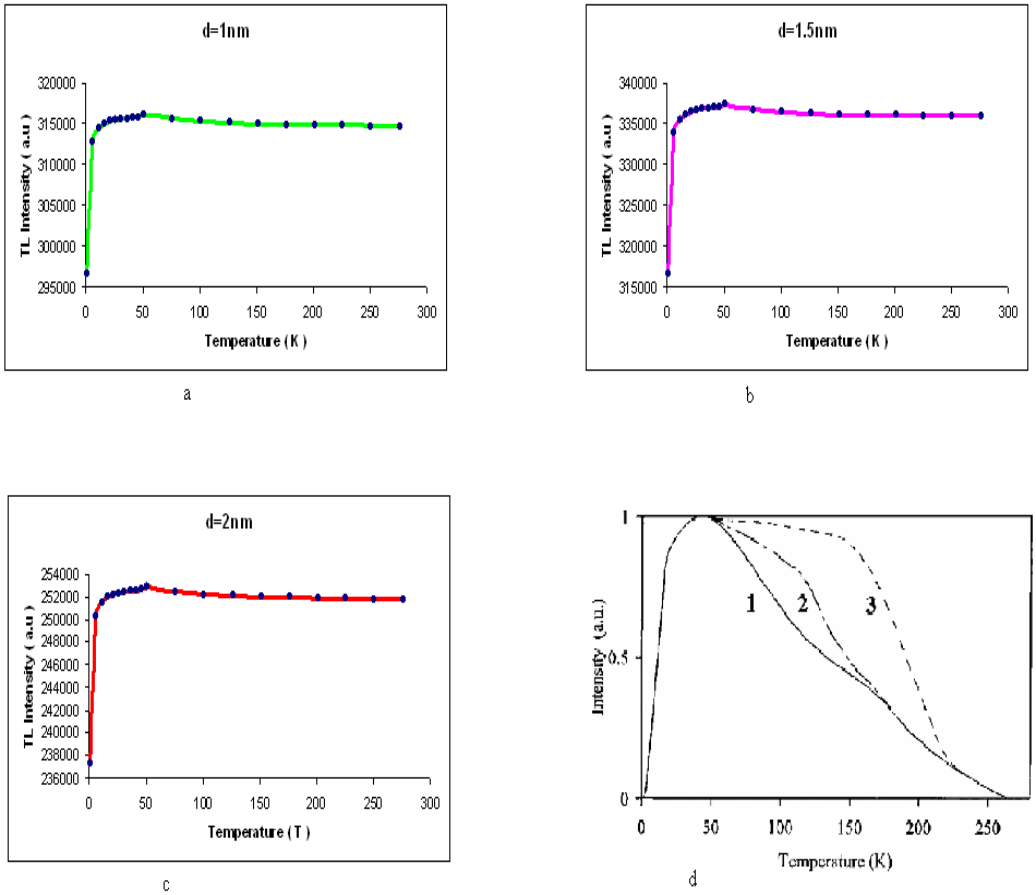


Figure 4.2: The calculated TL intensity for 1nm (a), 1.5nm (b), and 2nm (c) size samples. The experimental plot is also shown (d): ( model 2 ).

For a fixed value of b (which is approximately equal to -1.5) the thermoluminescence intensity has a peak value again at a temperature of 50K and starts decreasing after

this temperature. Also in this model we have worked for 1-300K temperature range and found out that our result is in good agreement with the experimental results. As it can be seen from the graphs ((a),(b) and (c)), the TL intensity increases with temperature and attains its maximum value near 50K and slowly decreases after this temperature. However, as compared to the experimental result ((d) ), the TL intensity obtained from this model decays much slower after a temperature of 50K (similar to model 1). Unlike model 1, there are no sharp peaks observed here and this may be due to the slight difference in the expressions for the two models.
This theoretical model is also in good agreement with the experimental results for temperatures lower than 1K. For such lower temperatures, the exponential term approaches zero and hence the TL intensity drops to zero.

Generally it is much interesting for us that both models converged to the same result regardless of the different approaches we made during derivations of these models. In fact there is a difference in the values of the constants in the final expressions of the models. But this doesn't make any significant difference in the basic shapes of the graphs and that is why we took both constants to be 1. Because of the $d^3$ dependence, model 2 gives enhanced TL intensity as compared to model 1 for sample size greater than $1nm$. But for sample size less than 1nm, model 1 gives enhanced TL intensity. The fact that the TL intensity increases following the reduction in nanoparticle size shows that quantum confinement effect is playing major role in allowing direct band to band radiative recombination.

## 4.3 Results for TL intensity versus size: model 1

We are also interested in calculating the TL intensity as a function of the size of the dot for a given temperature. As expected, we observed that for a given temperature, the TL intensity increases with decreasing the size. (see figure 4.4a, 4.4b and 4.4c) .

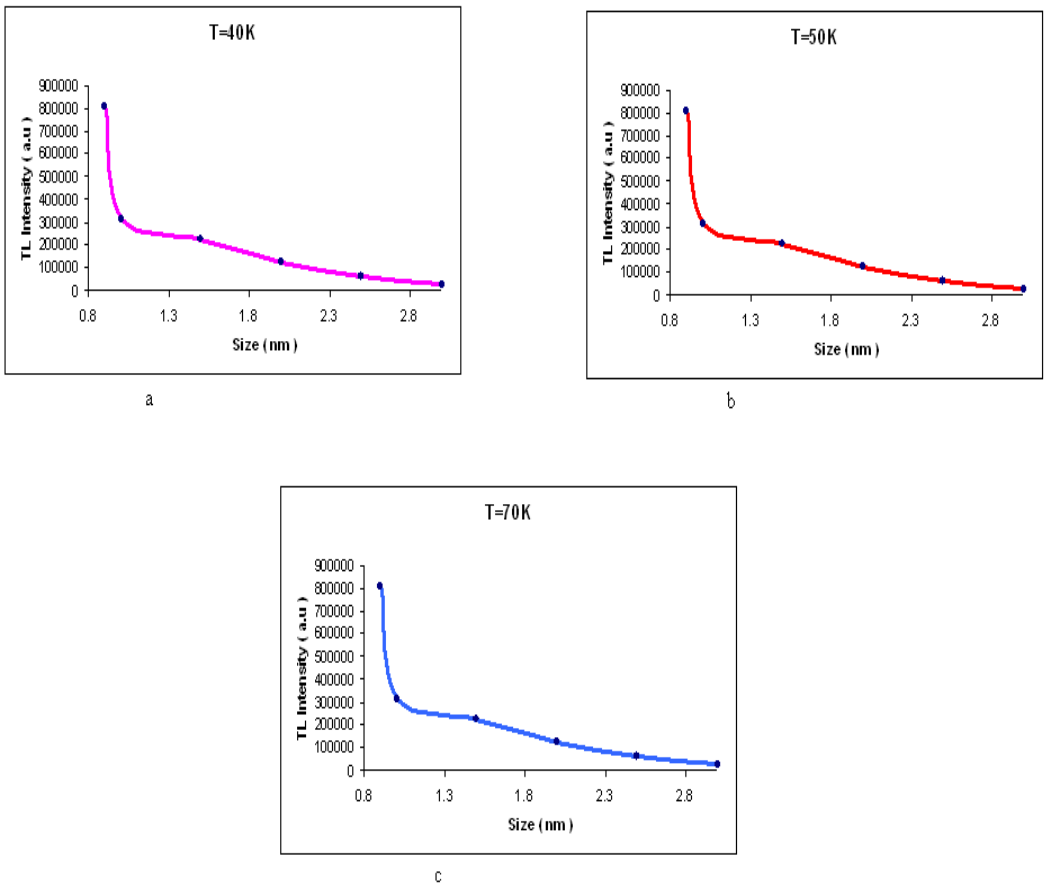


Figure 4.3: The calculated TL intensity versus size at different temperatures.

This is also due to the the quantum confinement effect which allows direct band to band radiative recombination following the widening of band gap. From this result one can easily understand that the TL intensity increases with increasing the band gap of the dot; because the reduction in size allows the increment of band gap.

## 4.4 Results for TL intensity versus size: model 2

The TL intensity obtained for model 2 is almost similar to that obtained from model 1. But for a fixed temperature, model 2 gives enhanced TL intensity. Of course, since the data of both models for TL intensity versus size are much closer to each other, it is difficult to distinguish between the two graphs.

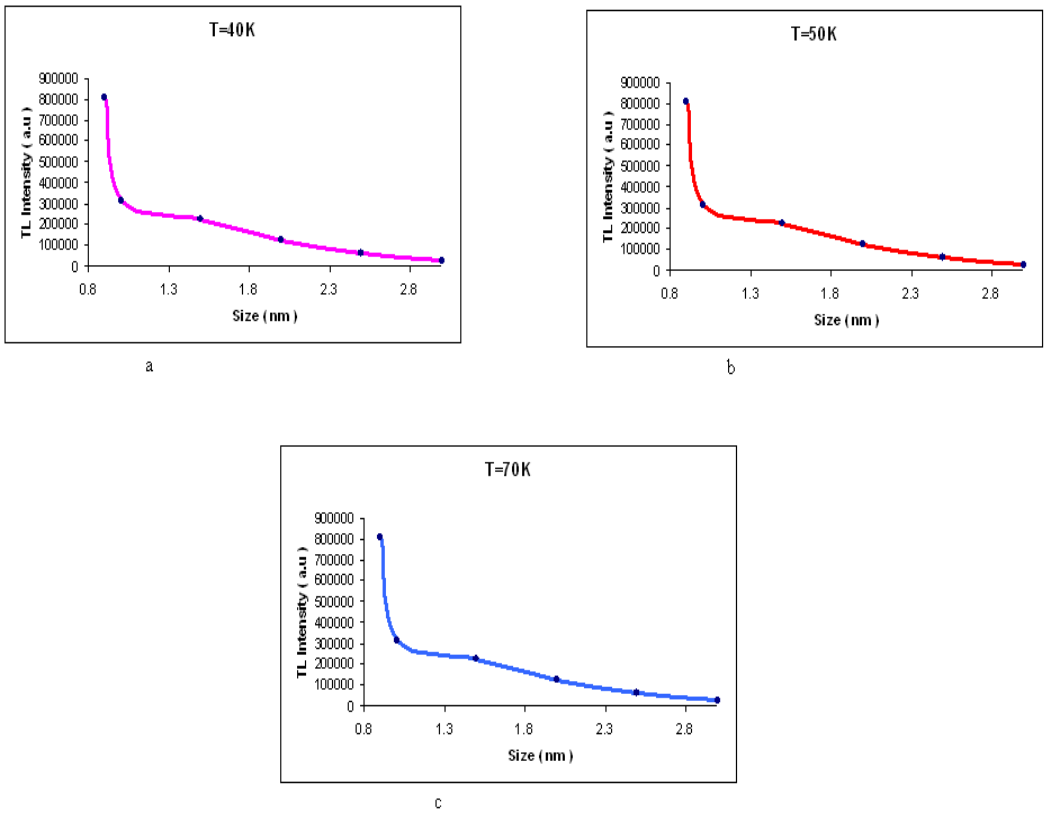


Figure 4.4: The calculated TL intensity versus size at different temperatures.

## 4.5 Results for the size dependent activation energy

For the first time we calculated the size dependent activation energy for a given temperature near temperature corresponding to the maxima of the curve and observed much interesting results. We have also calculated the size dependent activation energy at room temperature.

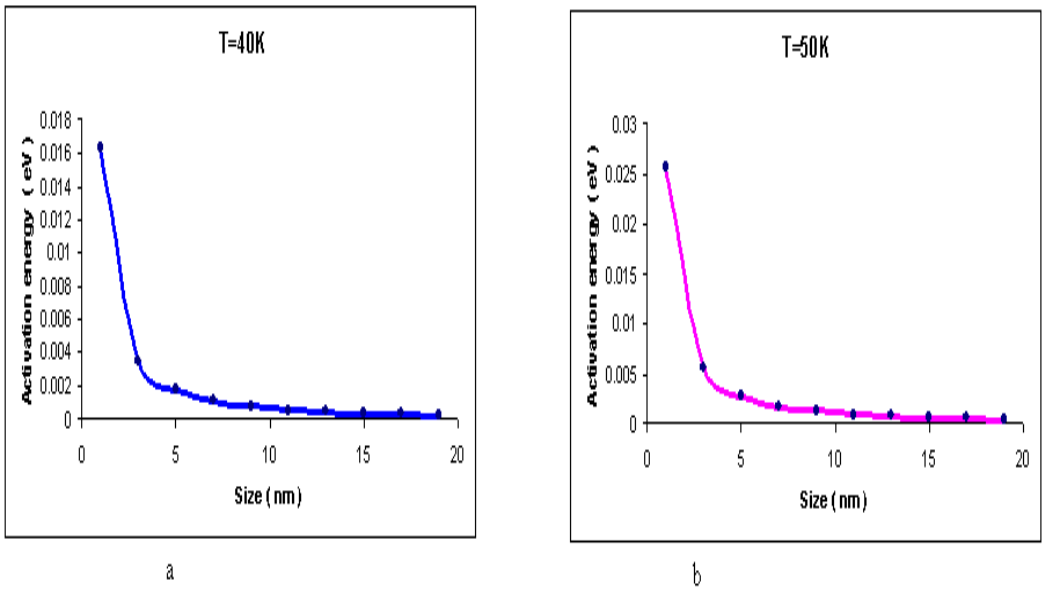


Figure 4.5: The calculated activation energy versus size for T=40K (a)and T=50K (b).

For $b = 1.99$, we observed from the calculated data that the activation energy increases with decreasing the size of the dot as expected. It is this phenomena that we can observe from the graphs ((a), (b), (c) and (d)). This indicates that the probability for the trap centers to be located at the deeper states will be higher following the reduction in size (increment of band gap). Also, in this model for size dependent activation energy, quantum confinement effect is playing a major role in increasing

the band gap and allowing the trap centers to be located in a more deeper states.

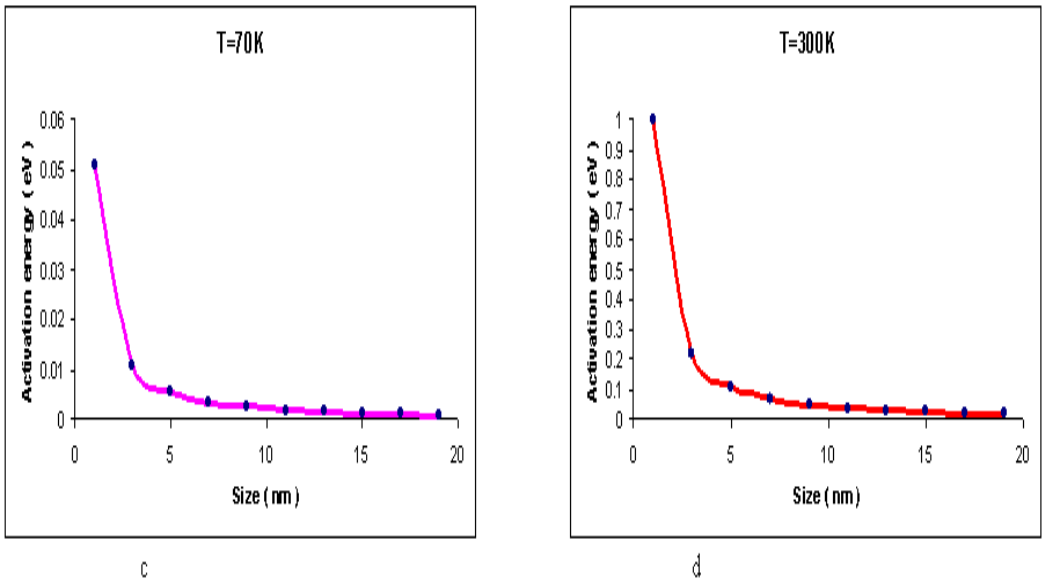


Figure 4.6: The calculated activation energy versus size for T=70K (c) and T=300K (d).

## 4.6 Results for the temperature dependent activation energy

For different sizes, we have also calculated the temperature dependent activation energy (trap depth) for the temperature range of 1-300K and for $b = 1.99$ (See figure 4.7a, 4.7b and 4.7c). Here our result is also in conformity with the experimental result (see figure 4.7d). From the calculated data and from the graphs, we observed that the activation energy increases with increasing temperature. It is also much interesting to observe that, for a given temperature, smaller dot has higher activation energy than relatively larger dot.

This effect can be explained in terms of quantum confinement effect. The smaller the

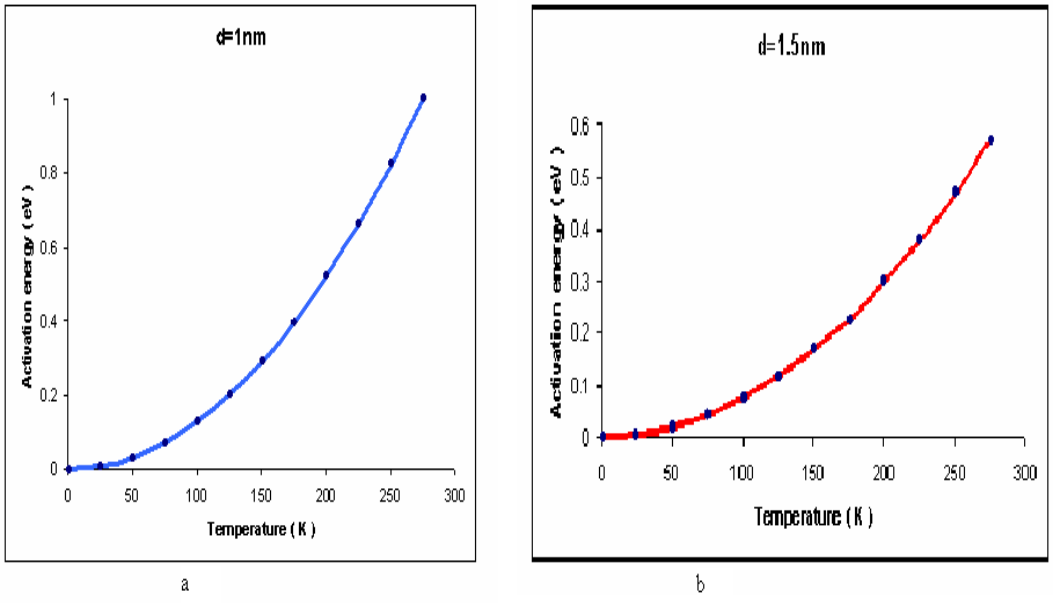


Figure 4.7: The calculated activation energy versus temperature for d=1nm (a) and d=1.5nm (b).

size of the dot, the wider the band gap. This increases the probability of the trap states to be located in the more deeper states for the relatively smaller dot than for the larger one at a given temperature. Hence, at a given temperature, the smaller dot has relatively higher activation energy than the bigger one. From the graphs it is important to note that, as compared to the experimental result, our model for calculating activation energy underestimates the value of activation energy for a given size and temperature. This may also be because of the simplicity of our theoretical model.

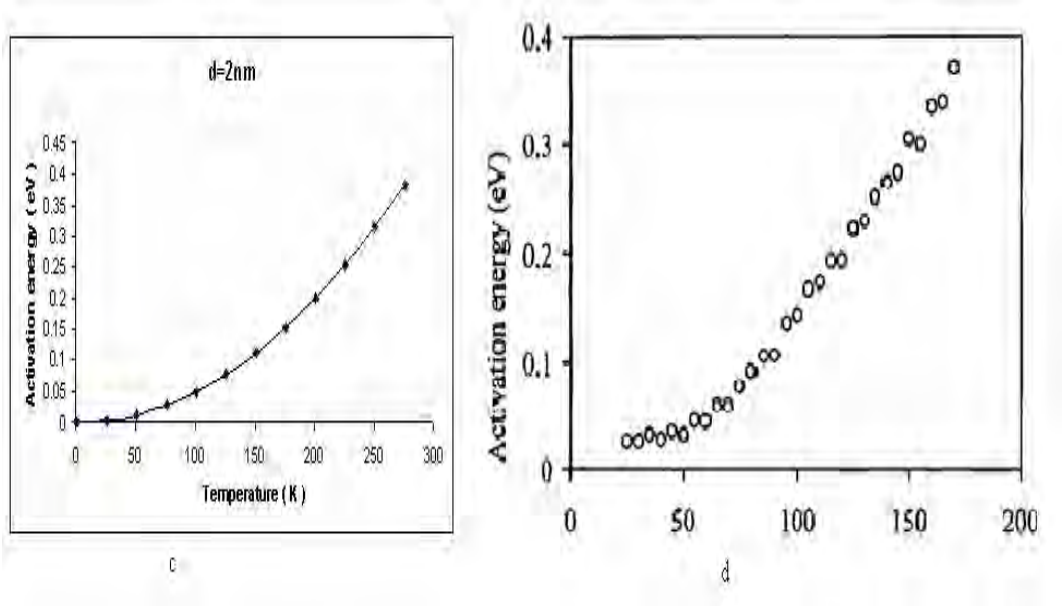


Figure 4.8: The calculated activation energy versus temperature for d=2nm (c) and the experimental plot (d).

# Chapter 5

# Conclusion and future outlook

## 5.1 Conclusion

In this work we have developed different models for calculating the TL intensity as a function of temperature, activation energy as a function of temperature and size. In model 1, for temperature dependent TL intensity, we tried to include some concepts from bulk material and obtained the expression for the TL intensity from the dot with some possible modifications. We observed that our result for this model is in good agreement with the experimental results. Therefore, this model has shown that applying the concept of bulk material is sometimes very important to understand the new behaviors reflected by materials at nanolevel. We can say that both model 1 and model 2 are powerful approaches for calculating the temperature dependent TL intensity. Of course both models have some limitations. We couldn't observe the fast decay mechanism of the TL intensity after 50K as the experimental result.

Luminescence can result because of two cases. One is due to the recombination of free electrons with trapped holes and the other is due to the recombination of free holes with trapped electrons. But in this work we have worked for the first case.i.e. luminescence due to the recombination of free electrons with trapped holes.

We have also calculated the size dependent TL intensity and observed that it increases

with decreasing the size of the dot. This is because of the fact that decreasing the size changes the band gap from indirect to direct and increases and band to band radiative recombination.

Moreover, we observed that there is very good match between the result of model for temperature dependent activation energy and the experimental result. But our model underestimates the value of the activation energy for a given size and temperature. In addition our result for size dependent activation energy is quite new and needs future investigations.

All the results we obtained from the our models can be explained well by the quantum confinement effect which allows band gap widening and direct band to band radiative recombination following the reduction in size.

As mentioned above , some of our results are quite new and can also be applied to Ge, GaAs etc nanoparticles.

In general we have observed that the temperature dependence of the TL intensity is much similar to that of the PL and EL intensities. This shows that the mechanism of luminescence in the three types of luminescence is in general similar to one another.

## 5.2 Some application of thermoluminescence

The absorption of radiation increases the level of thermoluminescence observed from a specimen by filling the localized energy levels with trapped electrons. The absorption of heat from the environment, on the other hand, tends to reduce the numbers of trapped electrons by thermally releasing them. Thus, the intensity of thermoluminescence a competition between trap filling by radiation and trap emptying by thermal excitation. At a given temperature of irradiation, many materials display an intensity of thermoluminescence which is proportional (or nearly so) to the amount of

radiation absorbed, and this leads to the fact that thermoluminescence may be used as a means of radiation dosimetry.

## 5.3 Future outlook

There are many papers/articles published each year on phenomena relating to thermoluminescence (generally termed thermally stimulated relaxations) and at this rate even more articles will be published in the future. This high rate of publication is surprising and it is reinforced because, as an experimental technique, thermoluminescence finds favor in such diverse scientific disciplines as archaeology, geology, medicine, solid state physics, biology and organic chemistry, to name just some of the main stream areas of study. In addition more will be done on how the thermoluminescence characteristics of a material is directly related to the materials solid state properties and how these solid state properties are being utilized in the diverse fields mentioned above.

# Appendix

Under this section, we put the FORTRAN code we used to generate our data. 'd' is the size of the sample and 'r' represents the corresponding radiative recombination rate.

```
c This program computes the TL intensity as function of temperature
c for a sample of 1nm in size (model 1)
real I
integer T
d=1
r=10**5.5
open(1,file='neb13.dat',status='unknown')
do T=1,50,5
I=r*(d**2)*exp(-0.064/T)
write(1,*) T,I
print*,T,I
end do
do T=51,300,25
I=r*(d**2)*exp(-((0.0058*T)-0.28)/T)
write(1,*) T,I
print*,T,I
end do
```

```
end
c This program computes the TL intensity as function of temperature
c for a sample of 1.5nm in size ( model 1 )
real I
integer T
d=1.5
r=10**5
open(1,file='neb12.dat',status='unknown')
do T=1,50,5
I=r*(d**2)*exp(-0.064/T)
write(1,*) T,I
print*,T,I
end do
do T=51,300,25
I=r*(d**2)*exp(-((0.0058*T)-0.28)/T)
write(1,*) T,I
print*,T,I
end do
end
c This program computes the TL intensity as function of temperature for
c a sample of 2nm in size ( model 1 )
real I
integer T
d=2
r=10**4.5
open(1,file='neb13.dat',status='unknown')
do T=1,50,5
```

```
I=r*(d**2)*exp(-0.064/T)
write(1,*) T,I
print*,T,I
end do
do T=51,300,25
I=r*(d**2)*exp(-((0.0058*T)-0.28)/T)
write(1,*) T,I
print*,T,I
end do
end
c This program computes the TL intensity as function of temperature for
c a sample of 1nm in size ( model 2 )
real I
integer T
d=1
r=10**5.5
open(1,file='2neb11.dat',status='unknown')
do T=1,50,5
I=r*(d**3)*exp(-0.064/T)
write(1,*) T,I
print*,T,I
end do
do T=51,300,25
I=r*(d**3)*exp(-((0.0058*T)-0.28)/T)
write(1,*) T,I
print*,T,I
end do
```

```
end
c This program computes the TL intensity as function of temperature for
c a sample of 1.5nm in size ( model 2 )
real I
integer T
d=1.5
r=10**5
open(1,file='2neb12.dat',status='unknown')
do T=1,50,5
I=r*(d**3)*exp(-0.064/T)
write(1,*) T,I
print*,T,I
end do
do T=51,300,25
I=r*(d**3)*exp(-((0.0058*T)-0.28)/T)
write(1,*) T,I
print*,T,I
end do
end
c This program computes the TL intensity as function of temperature
c for a sample of 2nm in size ( model 2 )
real I
integer T
d=2
r=10**4.5
open(1,file='2neb13.dat',status='unknown')
do T=1,50,5
```

```
I=r*(d**3)*exp(-0.064/T)
write(1,*) T,I
print*,T,I
end do
do T=51,300,25
I=r*(d**3)*exp(-((0.0058*T)-0.28)/T)
write(1,*) T,I
print*,T,I
end do
end
c this program computes the activation energy as function of size
c d at temperature T=40K
real E
Integer T
open(1,file='nact11.dat',status='unknown')
b=1.99
T=40
do d=1,20,2
y=d**1.39
z=3.73/y
E=z*(2+4*T+sqrt((2+4*T)**2-4*T*(2*T*(1-b)*alog(T)+3)))/2*T
write(1,*)d,E
print*,d,E
end do
end
c this program computes the activation energy as function of size d
c at temperature T=50K
```

```
real E
Integer T
open(1,file='nact12.dat',status='unknown')
b=1.99
T=50
do d=1,20,2
y=d**1.39
z=3.73/y
E=z*(2+4*T+sqrt((2+4*T)**2-4*T*(2*T*(1-b)*alog(T)+3)))/2*T
write(1,*)d,E
print*,d,E
end do
end
c this program computes the activation energy as function of size
c d at temperature T=70K
real E
Integer T
open(1,file='nact13.dat',status='unknown')
b=1.99
T=70
do d=1,20,2
y=d**1.39
z=3.73/y
E=z*(2+4*T+sqrt((2+4*T)**2-4*T*(2*T*(1-b)*alog(T)+3)))/2*T
write(1,*)d,E
print*,d,E
end do
```

```
end
c this program computes the activation energy as function of size
c d at temperature T=300K
real E
Integer T
open(1,file='nact14.dat',status='unknown')
b=1.99
T=300
do d=1,20,2
y=d**1.39
z=3.73/y
E=z*(2+4*T+sqrt((2+4*T)**2-4*T*(2*T*(1-b)*alog(T)+3)))/2*T
write(1,*)d,E
print*,d,E
end do
end
c this program computes the activation energy as function of
c temperature T for a give size d
c for d=1nm, the energy upshift (z)=3.73, for d=1.5nm, z=2.123,
c for d=2nm, z=1.423
real E
Integer T
open(1,file='nact1.dat',status='unknown')
b=1.99
z=3.73
do T=1,300,25
E=z*(2+4*T+sqrt((2+4*T)**2-4*T*(2*T*(1-b)*alog(T)+3)))/2*T
```

```
write(1,*)T,E
print*,T,E
end do
end
c this program computes the activation energy as function of
c temperature T for a give size d
c for d=1nm, the energy upshift (z)=3.73, for d=1.5nm, z=2.123,
c for d=2nm, z=1.423
real E
Integer T
open(1,file='nact2.dat',status='unknown')
b=1.99
z=2.123
do T=1,300,25
E=z*(2+4*T+sqrt((2+4*T)**2-4*T*(2*T*(1-b)*alog(T)+3)))/2*T
write(1,*)T,E
print*,T,E
end do
end
c this program computes the activation energy as function of temperature T
c for a give size d
c for d=1nm, the energy upshift (z)=3.73, for d=1.5nm, z=2.123,
c for d=2nm, z=1.423
real E
Integer T
open(1,file='nact3.dat',status='unknown')
b=1.99
```

```
z=1.423
do T=1,300,25
E=z*(2+4*T+sqrt((2+4*T)**2-4*T*(2*T*(1-b)*alog(T)+3)))/2*T
write(1,*)T,E
print*,T,E
end do
end
```

# Bibliography

[1] S. W. S Mckeever, Thermoluminescence of Solids, Cambridge solid state science series, Oklahoma state university, 396, (1988).

[2] S. Tripathy, R. K. Soni, S. K. Ghoshal and K. P. Jain, Bull. Mater. Sci. **24**, 285, (2005).

[3] Zhiyong Zhou, Michael L. Steigeward, Richard A. Frienser, and Louis Brus, Phys. Rev. B, **71**, 1, (2005).

[4] Yoshihiko Kanemitsu, Hiroshi Uto, and Yasuaki Masumoto, Phys. Rev. B, **48**, 2827, (1993).

[5] Toshihide Takagahara and Kyozaburo Takeda, Phys. Rev. B, **46**, 15578, (1992).

[6] L. Tsybeskov, E. K. Lee, H.-Y. Chang, B. V. Kamenev, D. J. Lockwood, J.-M. Baribeau, and T. I. Kamins, Hindawi Publishing Corporation, **10.1155/2008/218032**, 1, (2008).

[7] U. Pal, R. Melendrez, V. Chernov, and M. Barboza-Flores, Appl. Phys. Lett., **89**, 1, (2006).

[8] Claudo Furetta, Hand book of thermoluminescence Cambridge university press, 480.

[9] Kengo Nishio, Junichiro Koga, Toshio Yamaguchi and Fumiko Yonezawa, Phys. Rev. B, **67**, 1, (2003).

[10] Lin-Wang Wang and Alex Zunger, J. Chem. Phys. **100**, 2394, (1994).

[11] S. K. Ghoshal, Devendra Moham, Tadesse Tenaw Kassa and sunita Sharma, International J. Mod. Phys. B, **21**, 3783, (2007).

[12] P. Fillard and M.Castagne, Appl. Phys. Lett., **39**, 769, (1981).

[13] Julie Suzanne Biteen, and Harry A. Atwater, Thesis on Plasmon-enhanced silicon nanocrystal luminescence for optoelectronic application, (2006).

[14] Charles Kittle, An Introduction to Solid State Physics, Seventh edition, 673.

[15] Tae-Youb Kim, Nae-Man Park, Kyung-Hyun Kim, Young-Woo Ok, Tae-Yeon Seong, Cheo- Jong Choi and Gun Yong Sung, Mat. Res. Soc. Symp. Proc. **817**, (2004).

[16] J. I. Pankove, Optical Processes in Semiconductors, Prentice-Hall, Englewood Cliffs, New Jersey, 452, (1971).

[17] Karl W. Boer, Survey of Semiconductor Physics: Electrons and Other Particles in Bulk Semiconductors, Nostrand Reinhold, 1423, (1990).

[18] Jasprit Singh: www.eecs.umich.edu/Singh, John-Wiley, 2001.

[19] M. Grayson, D. C. Tsui, and M. Shayegan, Appl. Phys. Lett., **67**, 1564, (1995).

[20] Yu. A. Skryshevskii, and V. A. Skryshevskii, J. Appl. Phys., **89**, 2711, (2001).

# DECLARATION

I here under signed declare that the thesis is my original work, has not been presented for a degree in any other university and that all sources of material used for the thesis have been dully acknowledged.

Name: Nebiyu Gemechu

Signature:———————————

This thesis has been submitted for examination with my approve as a university advisor.

Name: S. K. Ghoshal

Signature:———————————